

December 2013

Arabidopsis SERK1 and 2 Regulate Anther Development as Co-Receptors of EMS1

Yao Wang

University of Wisconsin-Milwaukee

Follow this and additional works at: <https://dc.uwm.edu/etd>

 Part of the [Plant Biology Commons](#)

Recommended Citation

Wang, Yao, "Arabidopsis SERK1 and 2 Regulate Anther Development as Co-Receptors of EMS1" (2013). *Theses and Dissertations*. 777.
<https://dc.uwm.edu/etd/777>

This Dissertation is brought to you for free and open access by UWM Digital Commons. It has been accepted for inclusion in Theses and Dissertations by an authorized administrator of UWM Digital Commons. For more information, please contact open-access@uwm.edu.

***Arabidopsis* SERK1 AND 2 REGULATE ANTHOR
DEVELOPMENT AS CO-RECEPTORS OF EMS1**

by

Yao Wang

A Dissertation Submitted in

Partial Fulfillment of the

Requirement for the Degree of

Doctor of Philosophy

in Biological Sciences

at

The University of Wisconsin – Milwaukee

May 2014

ABSTRACT

***Arabidopsis* SERK1 AND 2 REGULATE ANTHER DEVELOPMENT AS CO-RECEPTORS OF EMS1**

by

Yao Wang

The University of Wisconsin-Milwaukee, 2014

Under the Supervision of Da-Zhong Zhao, Ph.D.

In flowering plants, male reproductive cell differentiation, one of the most critical events in the early stage of sexual reproduction, occurs during anther development. In the model plant species *Arabidopsis*, anther development in each lobe results in the differentiation of five highly organized cell layers with unique identities, including the central male reproductive cells and four somatic cell layers. These features make the *Arabidopsis* anther an ideal system in which to investigate the mechanisms of cell fate determination and differentiation. Previous studies have demonstrated that a leucine-rich repeat receptor-like kinase (LRR-RLK), EXCESS MICROSPOROCTES1 (EMS1/EXS1), plays an important role during *Arabidopsis* anther development. In this study, we provided both genetic and biochemical evidence showing that two additional LRR-RLKs, SERK1 and SERK2, are also involved in the regulation of anther cell development as co-receptors of EMS1.

In our genetic studies, based on a recently identified weak allele of *EMS1*, *ems1-2*, we first showed that *EMS1* and *SERK1/2* interact with each other genetically, as indicated by the sterile phenotype of *ems1-2 serk1-1* double mutant. We then showed that *EMS1* and *SERK1/2* function in the same genetic signaling pathway. The full function of

EMS1 is dependent on *SERK1/2* expression, which suggests that *SERK1/2* may work as co-receptors of *EMS1*. We also used complementation experiments to show a partial functional redundancy between *SERK1* and *SERK2*. Moreover, *SERK1* seems to be more important functionally during *Arabidopsis* anther development due to its biochemical nature, as reflected by its stronger autophosphorylation level compared with *SERK2* during the *in vitro* kinase assay.

In biochemical studies focusing on *SERK1* and *EMS1*, we showed that *EMS1* specifically interacts with *SERK1* in the bimolecular fluorescent complementation (BiFC) assays using *Arabidopsis* protoplasts. We also made truncated versions of *EMS1* and *SERK1* in order to narrow down the particular regions responsible for the interaction.

In addition, we demonstrated the significance of *EMS1* phosphorylation during the interaction of *EMS1* and *SERK1*. We showed that transphosphorylation between *EMS1* and *SERK1* enhanced the phosphorylation levels of both proteins. Also, multiple serines and threonines were detected as phosphorylation sites in our *in vitro* mapping effort within the kinase domain of *EMS1*.

In summary, this study provides both genetic and biochemical evidence suggesting that *SERK1/2* regulate *Arabidopsis* anther cell development as co-receptors of *EMS1*. Phosphorylation of multiple serine/threonine residues in the *EMS1* kinase domain is critical for the physiological function of *EMS1*.

Table of Contents

	Page
Abstract.....	ii
Table of Contents.....	iv
List of Abbreviations.....	x
List of Figures.....	xii
List of Tables.....	xiv
Acknowledgments.....	xv
 Chapter 1: Introduction	
1.1 Introduction.....	1
1.1a <i>Arabidopsis</i> anther, a model system.....	1
1.1b Anther developmental stages in <i>Arabidopsis</i>	2
1.1c Genetic control of floral organ and stamen identity in <i>Arabidopsis</i>	3
1.1d Multiple functional roles of <i>Arabidopsis</i> LRR-RLKs.....	4
1.1e <i>Arabidopsis</i> LRR-RLKs regulate anther development.....	6
1.1f The <i>EMS1</i> signaling pathway is essential for anther development in <i>Arabidopsis</i>	8

1.1g SERK1 and SERK2 are involved in the regulation of <i>Arabidopsis</i> anther cell differentiation, possibly together with EMS1.....	10
-----------------------------------------------------------------------------------------------------------------------------------------	----

1.2 Research Objectives.....	11
------------------------------	----

Chapter 2: Materials and Methods

2.1 Strains, plasmids, primers and chemicals.....	14
---------------------------------------------------	----

2.1.1 Strains: storage, cultures and transformation.....	14
----------------------------------------------------------	----

2.1.2 Plasmids and primers.....	15
---------------------------------	----

2.2 Genetic Studies

2.2a Plant materials and growth conditions.....	24
-------------------------------------------------	----

Identification of new <i>ems1</i> and <i>serk1/2</i> T-DNA lines.....	24
-----------------------------------------------------------------------	----

RT-PCR examination of gene expression in the <i>ems1-2</i> line.....	25
----------------------------------------------------------------------	----

Genotyping of <i>Arabidopsis</i> T-DNA and Ds lines.....	25
----------------------------------------------------------	----

Plant genomic DNA extraction

PCR examination of genetic background

Generation of <i>Arabidopsis</i> double/triple mutant lines.....	27
------------------------------------------------------------------	----

Crosses of *Arabidopsis* plants

Double/triple *Arabidopsis* mutant line generation

2.2b Phenotypic analysis.....	28
-------------------------------	----

Plant fertility loss evaluation.....	28
--------------------------------------	----

	Page
Pollen staining examination.....	29
2.2c Semi-thin section analysis of <i>Arabidopsis</i> inflorescences.....	29
Fixation, post-fixation, dehydration and resin infiltration	
Sample dissection and embedding	
Semi-thin sectioning	
2.2d <i>Arabidopsis</i> plant transformation.....	31
2.2e <i>Arabidopsis</i> transformant analysis.....	32
2.3 Biochemical Studies	
2.3a Examination of EMS1 and SERK1 interaction using BiFC.....	32
Plasmid Construction and preparation for BiFC.....	33
Preparation of <i>Arabidopsis</i> protoplasts.....	34
Transfection of <i>Arabidopsis</i> protoplasts.....	35
2.3b Preparation for co-immunoprecipitation of EMS1 and SERK1 in	
<i>Arabidopsis</i> anthers.....	35
Plasmid construction for SERK1 protein expression in <i>Arabidopsis</i>.....	36
SERK1 transformant generation and screening.....	36
Generation of <i>EMS1::EMS1-cMyc /ems1-2 serk-1</i> plants.....	37
2.4 Functional phosphorylation analysis of EMS1	

2.4a Identification of <i>in vitro</i> phosphorylation residues within the EMS1 kinase domain.....	37
Plasmid construction for GST-EMS1-KD fusion protein expression.....	37
GST-EMS1-KD recombinant protein expression and purification.....	38
<i>In vitro</i> autophosphorylation assay of GST-EMS1-KD protein.....	40
2.4b <i>In vitro</i> transphosphorylation between kinase domains of EMS1 and SERK1	
Plasmid construction for His-SERK1-KD fusion protein expression.....	40
His-SERK1-KD recombinant protein expression and purification.....	40
<i>In vitro</i> cross phosphorylation between His-SERK1-KD and GST-EMS1-KD recombinant proteins.....	42
Mutagenesis of His-SERK1-KD and GST-EMS1-KD recombinant proteins....	43
 Chapter 3: Results	
 3.1 <i>EMS1</i> genetically interacts with <i>SERK1</i>	45
3.1a Identification of the <i>EMS1</i> weak allele, <i>ems1-2</i>.....	45
3.1b <i>ems1-2 serk1-1</i> double mutants showed significantly fertility reduction....	47
3.1c <i>ems1-2 serk1-1</i> double mutants showed defects in anther cell development.....	53

3.1d <i>ems1 serk1-1 serk2-1</i> triple mutants showed anther phenotype identical to <i>ems1</i> and <i>serk1-1 serk2-1</i>	55
3.1e <i>EMS1</i> signaling is dependent on <i>SERK1/2</i> function.....	56
3.1f <i>SERK1</i> and <i>SERK2</i> play partially redundant yet unequally important roles during anther development in <i>Arabidopsis</i>	58
3.2 <i>SERK1</i> biochemically interacts with <i>EMS1</i> in <i>Arabidopsis</i>	
3.2a <i>SERK1</i> specifically interacts with <i>EMS1</i> in <i>Arabidopsis</i> protoplasts.....	60
3.2b Interaction between truncated <i>EMS1</i> and <i>SERK1</i> in <i>Arabidopsis</i> protoplasts	61
3.2c The ligand protein <i>TPD1</i> is not required for <i>SERK1-EMS1</i> interaction in <i>Arabidopsis</i> protoplasts.....	63
3.2d Homodimerization observed between <i>SERK1</i> but not <i>EMS1</i> proteins in <i>Arabidopsis</i> protoplasts.....	64
3.3 Functional analysis of <i>EMS1</i> phosphorylation	
3.3a Transphosphorylation occurs between kinase domains of <i>EMS1</i> and <i>SERK1</i>	66
3.3b K945E mutation does not abolish in vitro autophosphorylation activity in GST- <i>EMS1-KD</i>	67
3.3c Identification of in vitro phosphorylation sites within GST- <i>EMS1-KD</i>	68

Chapter 4: Discussion

4.1 Redundancy between SERK1 and SERK2.....72

4.2 Role of TPD1 during EMS1-SERK1/2 interaction.....74

4.3 Working model of the EMS1-SERK1/2 protein complex.....75

4.4 Phosphorylation within the EMS1 kinase domain.....76

4.5 Potential molecules downstream of EMS1 signaling.....78

Chapter 5 Conclusions and Future Directions

5.1 Conclusion.....80

5.2 Directions for future studies.....81

References.....83

CURRICULUM VITAE.....94

List of Abbreviations

½ MS media	½ Mursashige & Skoog (basal salt mixture) media
AG	AGAMOUS
Amp	Ampicillin
AP3	APETALA3
BAK1	BRI1-ASSOCIATED RECEPTOR KINASE1
BiFC	Bimolecular fluorescent complementation
BR	Brassinosteroids
BRI1	BRASSINOSTEROID-INSENSITIVE 1
EMS1/EXS1	EXCESS MICROSPOROCTES1
EYFP	Enhanced yellow fluorescent protein
HEPES	4-(2-hydroxyethyl)-1-piperazineethanesulfonic acid
HmB	Hygromycin B
IPTG	Isopropyl β-D-1-thiogalactopyranoside
Kan	Kanamycin
LB medium	Luria-Bertani medium
LC/MS/MS	Liquid chromatography-tandem mass spectrometry

List of Abbreviations (continues)

<i>Ler</i>	Landsberg <i>erecta</i> (an <i>Arabidopsis</i> ecotype)
LRR-RLK	Leucine-rich repeat receptor-like kinase
PEG	polyethylene glycol
PI	PISTILLATA
RPK2	RECEPTOR-LIKE PROTEIN KINASE 2
RPM	round per minute
SERK1/2	SOMATIC EMBROGENESIS RECEPTOR KINASE1/2
SDS-PAGE	Sodium dodecyl sulfate polyacrylamide gel electrophoresis
SPL	SPOROCTELESS
TPD1	TAPETUM DETERMINANT1

List of Figures

	Page
Fig 1.1 <i>Arabidopsis</i> anther structure.....	2
Fig 1.2 Proposed working model of the EMS1 protein complex in <i>Arabidopsis</i> anthers.....	11
Fig 2.1 <i>Arabidopsis</i> insertion mutant lines identified and used in this study.....	24
Fig 3.1 <i>ems1-2</i> is a weak allele of <i>EMS1</i>	46
Fig 3.2 <i>serk1-1 ems1-2</i> double mutants show significant fertility reduction.....	48
Fig 3.3 Fertility loss and recovery in <i>ems1-2 serk1-1</i> plants.....	50
Fig 3.4 <i>ems1-2 serk1-1</i> double mutant flowers show defects in pollen production	52
Fig 3.5 <i>ems1-2 serk1-1</i> double mutants are defective in anther cell development	54
Fig 3.6 <i>ems1 serk1-1 serk2-1</i> triple mutants show identical phenotype as <i>ems1</i> and <i>serk1-1 serk2-1</i>	55
Fig 3.7 <i>AtML1::TPD1</i> overexpression triggers abnormal anther cell proliferation in Col-0 wild type but not in <i>serk1-1 serk2-1</i> double mutants.....	57

Fig 3.8 SERK1 specifically interact with EMS1 in <i>Arabidopsis</i> protoplasts.....	61
Fig 3.9 Kinase domains are not essential for interaction between SERK1 and EMS1 in <i>Arabidopsis</i> protoplasts.....	62
Fig 3.10 SERK1 interacts with EMS1 in <i>Arabidopsis</i> protoplasts prepared from <i>tpd1</i> plants.....	64
Fig 3.11 SERK1 but not EMS1 proteins form homodimers in <i>Arabidopsis</i>.....	65
Fig 3.12 <i>In vitro</i> autophosphorylation and transphosphorylation of GST-EMS1-KD and His-SERK1-KD proteins (radioautography gel scanning).....	67
Fig 3.13 <i>In vitro</i> autophosphorylation activity is not disrupted after K945E mutation in GST-EMS1-KD (radioautography gel scanning).....	68
Fig 3.14 GST-EMS1-KD recombinant protein is phosphorylated on multiple serine/threonine residues <i>in vitro</i>.....	68
Fig 3.15 Quantitative enhancement of phosphorylation in GST-EMS1-KD protein after His-SERK1-KD transphosphorylation <i>in vitro</i>.....	70

List of Tables

	Page
Table 2.1 <i>E.coli</i> and <i>Agrobacterium tumefaciens</i> strains used in this study.....	14
Table 2.2 Plasmids used in this study.....	15
Table 2.3 Primers used in this study.....	18
Table 3.1 Complementation effect of <i>SERK1::SERK2</i> and <i>SERK2::SERK1</i> in <i>serk1-1 serk2-1</i> background.....	57
Table 3.2 Complementation effect of <i>SERK1::SERK2</i> and <i>SERK2::SERK2</i> in <i>ems1-2 serk1-1</i> background.....	57

Acknowledgement

I would like to first give my sincere thanks and foremost appreciation to my advisor, Dr. Da-Zhong Zhao, whose inspiration and support has always been there throughout my entire graduate study. This work would not be possible without his encouragement and support.

I also would like to thank other members on my advisory committee, Dr. Heather Owen, Dr. Charles Wimpee, Dr. David Heathcote and Dr. Sergei Kuchin for their valuable discussions and helpful advice, as well as understanding and support. Furthermore, I particularly owe many thanks to Dr. Owen, who has helped me tremendously with all of my electron microscopy related works.

I would like to give special thanks to Jian Huang, our senior researcher, who has been a wonderful trainer and colleague since my first day in the lab. I greatly appreciate all the research assistance and support from Jian. I have been helped a lot from our discussions and his thoughtful advice during my research. I also would like to thank those previous and current members of our lab during my stay, for their support and help.

I would like to thank our collaborators who helped with the detection of the phosphorylated residues within the kinase domain of EMS1 protein during this work: Dr. Steve Clouse, Dr. Xiao-Feng Wang, Dr. Jay J. Thelen, Dr. Louis J. Meyer and Dr. Nagib Ahsan. Their fruitful work has been extremely helpful to us in understanding the

significance of EMS1 phosphorylation, and in revealing the mechanism of interaction between EMS1 and SERK1/2. Their contribution during our collaboration is highly appreciated.

I also would like to thank all the people from the department of biological sciences who helped my studies and researches a lot in different ways: Thomas Schuck, for his constant support work in maintaining our research facility; Phyllis Shaw and Dr. Jane L. Witten, for their help during my entire graduate studies; those professors who taught me, for their patient instructions; and all of the front desk people, for their daily assistance.

Last but not least, my deepest thanks go to those loving people from my family, my wife Miao Feng, my daughter Yu-Han Wang, and my parents in China, for their strong inspiration and support, for their warm care and love. I also could never have been able to finish this work without everything they have done for me. This work is dedicated to my father, who just passed away earlier in December.

Chapter 1: Introduction

1.1 Introduction

1.1a *Arabidopsis* anther, a model system

In flowering plants, the specification of male reproductive cells occurs during anther development (Goldberg et al., 1993; Scott et al., 2004; Sanders et al., 1999; Zhao et al., 2002; Jia et al., 2008). In the model plant species *Arabidopsis*, the typical structure of a developed anther consists of four lobes, with highly organized cell layers in each lobe. Five kinds of specialized cell types can be observed in each anther lobe (Figure 1.1). Microsporocytes, which are male reproductive cells, appear in the center of each anther lobe. Four surrounding somatic cell layers, tapetum, middle layer, endothecium and epidermis are arranged as individual ring-shaped circles, each a single cell thick, from innermost to outermost. As anther development represents the differentiation of multiple highly organized cell types, including the specification of male reproductive cells from somatic cells, the *Arabidopsis* anther emerges as a valuable model system for addressing many fundamental biological principles, particularly the molecular mechanisms underlying cellular signaling (Ma., 2005; Wijeratne et al., 2007; Zhao et al., 2002; Jia et al., 2008). However, the signaling network which regulates multiple aspects of anther cell differentiation and development still remains insufficiently understood, although considerable progress has been made in recent years (Zhao et al., 2002; Canales et al.,

2002; Yang et al., 2003; Albrecht et al., 2005; Colcombet et al., 2005; Mizuno et al., 2007; Hord et al., 2006; DeYoung et al., 2006; Zhao et al., 2008).

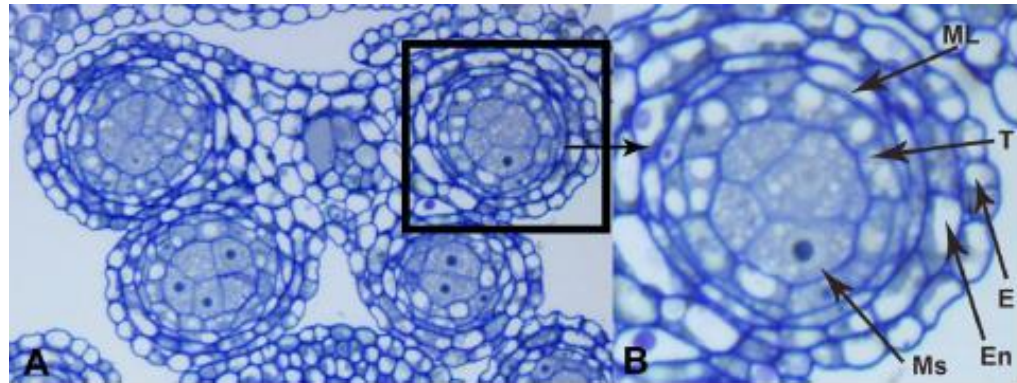


Fig1.1. *Arabidopsis* anther structure

(A) Semi-thin section of a wild type *Arabidopsis* anther in development stage 6.

(B) A magnified anther lobe (upper-right) showing five specified cell types, from inside to outside: Microsporocytes (Ms), tapetum (T), middle layer (ML), endothecium (En) and epidermis (E)

1.1b Anther developmental stages in *Arabidopsis*

In *Arabidopsis*, based on distinct cellular events that can be recognized by light microscopy, anther development has been described as a series of 14 stages (Sanders et al. 1999).

In stage 1, anther primordium emerge as round structures containing three cell layers, which will undergo further division in stage 2 and 3. In stage 4, as the result of

continuous cell divisions in anther primordium, the bilateral anther structure with four lobes is fully established with five distinct cell types. With sporogenous cells in the center, four surrounding somatic cell layers can be seen as tapetum, middle layer, endothecium and epidermis, from innermost to outermost. During stages 5 to 7, sporogenous cells undergo meiosis and generate microspores in the form of tetrads. After being released in stage 8 from tetrads, microspores further develop into pollen grains during stages 9 to 12. Dehiscence, the release of pollen grains from anther lobes, occurs at stage 13, after which the anther senesces and falls off from the plant. Pollen grains produce pollen tubes after their arrival at the stigma, which deliver sperm cells into the ovaries and trigger the double fertilization.

Stage 5 is a unique milestone among all anther developmental stages. It is when the reproductive cells separate from somatic cells within the anther.

1.1c Genetic control of floral organ and stamen identity in *Arabidopsis*

In *Arabidopsis*, multiple genes have been identified as regulators of floral organ identities in the four floral whorls. (Weigel et al., 1994; Ma., 2005) The identity of stamens is mainly controlled by homeotic genes *AGAMOUS* (*AG*) (Bowman et al., 1989, 1991a, b) and *PISTILLATA* (*PI*) (Gotoet et al., 1994; Krizek et al., 1996), both of which encode transcription factors. Mutation of either genes will trigger the homeotic conversion of stamens into other floral organs. The *AG* gene also limits stem cell proliferation in *Arabidopsis* flowers (Lohmann et al., 2001) and controls

microsporogenesis by activating the *SPOROCTELESS* gene (*SPL*) (Ito et al., 2004), which encodes a transcription factor. In the *spl* mutant, microsporocytes, as well as tapetum and endothecium, are not formed in the anthers (Yang et al., 1999; Schiefthaler et al., 1999).

Mutations in some other homeotic genes can also alter normal stamen identity. One such example is *APETALA3* (*AP3*) (Jack et al., 1992), which also encodes a transcription factor that is required for petal specification. Mutation of *AP3* leads to the homeotic transformation of stamens to carpels. By contrast, ectopic expression of *AP3* alters the expression domain of *PI*, triggering the replacement of carpels by stamens in the flowers (Jack et al., 1994).

1.1d Multiple functional roles of *Arabidopsis* LRR-RLKs

In the model plant species *Arabidopsis*, more than 200 genes encode leucine-rich repeat receptor-like kinases (LRR-RLKs), the largest family of *Arabidopsis* RLKs (Shiu et al., 2001; Torii 2004). A typical LRR-RLK protein has three main functional domains: an extracellular domain consisting of multiple leucine-rich repeats as ligand recognition and binding sites, a transmembrane domain that anchors the protein on the plasma membrane, and an intercellular kinase domain which controls autophosphorylation and transphosphorylation with other proteins. In *Arabidopsis* LRR-RLKs, kinase domains are highly conserved while LRR domains are variable in both length and sequence among different LRR-RLKs. Both the LRR and kinase domains are believed to be critical during

protein interactions. *Arabidopsis* LRR-RLKs had been described as serine/threonine kinases until a recent observation of tyrosine phosphorylation (Oh et al., 2009). Tyrosine phosphorylation is found to be responsible for controlling flowering time and releasing inhibitor protein in BRASSINOSTEROID-INSENSITIVE 1 (BRI1), one of the few well studied *Arabidopsis* LRR-RLKs (Oh et al., 2010; Jaillais et al., 2011).

Although the functions of most LRR-RLKs remain unclear currently, many of them have been found to play important roles in a wide range of growth and developmental events in *Arabidopsis*, such as cell fate determination (Zhao et al., 2002; Canales et al., 2002), meristem cell development regulation (Clark et al., 1997; DeYoung et al., 2006), hormone signaling (Li et al., 1997; Caño-Delgado et al., 2004), pathogen defense (Gomez-Gomez et al., 2000; Heese et al., 2007), organ abscission (Jinn et al., 2000), organ structure regulation (Torii et al., 1996) and flowering time regulation (Domagalska et al., 2007; Oh et al., 2010). In some other flowering plant species, such as rice and maize, LRR-RLK signaling pathways have been found to perform similar functions as those in *Arabidopsis* (Zhao et al., 2008; Sheridan et al., 1999).

In order to further uncover the signaling mechanisms of *Arabidopsis* LRR-RLKs, studies from multiple aspects have been performed. Researchers have used many different approaches, including identification of downstream/upstream signaling molecules (Wang et al., 2006), interacting partner screening (Nam et al., 2002; Jia et al., 2008), examinations of protein sub-cellular localization (Rojo et al., 2002; Bleckmann et al., 2010), identification of other LRR-RLKs with redundant functions (Caño-Delgado et

al., 2004; Müller et al., 2008), studies of phosphorylation mechanisms (Wang et al., 2005, 2008) and functional domain dissections (Kinoshita et al., 2005; Sun et al., 2012). The *Arabidopsis* LRR-RLKs are able to interact with multiple types of molecules, including plant hormones (Kinoshita et al., 2005), short peptide (Trotochaud et al., 2000), small proteins (Jia et al., 2008), RLKs (Müller et al., 2008) and other LRR-RLKs (Nam et al., 2002). Thus, *Arabidopsis* LRR-RLKs have a broad range of interacting molecules, which are essential pieces of the signaling pathways they mediate.

There are two major goals in the future studies of *Arabidopsis* LRR-RLKs. Larger numbers of LRR-RLKs will need to have their physiological functions characterized, to provide a clearer overall picture of the signaling networks in which they are involved. In addition, we need to know more details about the working mechanisms of LRR-RLKs as versatile regulators in order to understand how plants work and how they can be potentially manipulated for agricultural applications.

1.1e *Arabidopsis* LRR-RLKs regulate anther development

Several *Arabidopsis* LRR-RLKs have been reported as key regulators during anther cell differentiation and development. Mutation of these genes triggers a variety of developmental defects in anther cell layers that lead to male sterility.

In *rpk2* plants, the middle layer is missing in anther lobes (Mizuno et al., 2007). Pollen grains in *rpk2* anthers are abnormally sticky. Dehiscence failure in *rpk2* causes

male sterile phenotype. In addition, *rpk2* plants show some defects in vegetative growth, which suggests the possible multifunctional role of the *RPK2* gene in plants. A recent study revealed that *RPK2* is also involved in the signaling network which regulates meristem development in *Arabidopsis* (Kinoshita et al., 2010).

In another example, while the mutation of neither single gene disrupts normal anther development, simultaneous mutations of *BAM1* and *BAM2* show additive effects in anther lobes, which are poorly differentiated and do not develop following three cell layers: tapetum, middle layer and endothecium (Hord et al., 2006; DeYoung et al., 2006). The initial phenotype observed in *bam1 bam2* double mutants was loss of stem cells in the shoot and floral meristem. This is another piece of evidence indicating that many *Arabidopsis* LRR RLKs may serve in more than one signaling pathway.

The anthers in *ems1/exs1* plants produce excessive numbers of microsporocytes, but lack a developed tapetum (Zhao et al., 2002; Canales et al., 2002). Based on the number of microsporocytes in *ems1* anthers, a reasonable explanation is that those extra microsporocytes are derived from tapetum precursor cells, whose cell fate is altered due to the disruption of *EMS1* signaling.

An anther defective phenotype similar to that in *ems1* is also found in both *tpd1* and *serk1 serk2* double mutants (Yang et al., 2003; Albrecht et al., 2005; Colcombet et al., 2005). Notably, the *TPD1* gene encodes a small putative protein rather than a LRR-RLK. A recently study reported that TPD1 works as the ligand of EMS1 (Jia et al., 2008). Both *SERK1* and *SERK2* genes encode LRR-RLKs with a relatively shorter extracellular LRR

domain than other typical LRR-RLKs (Hecht et al., 2001; Shiu et al., 2001). There are five members in the *Arabidopsis* SERK protein family. Although SERK1 and SERK2 have been proposed as partners of EMS1 protein, only indirect evidence from genetic studies is currently available. Single mutants of either *SERK1* or *SERK2* show no defects in anther cell differentiation and development (Albrecht et al., 2005; Colcombet et al., 2005).

1.1f The *EMS1* signaling pathway is essential for anther development in *Arabidopsis*.

In *Arabidopsis*, the *EMS1* mediated signaling pathway plays an important role in regulating anther cell differentiation. Mutation of the *EMS1* gene leads to defective anthers showing abnormal cell differentiation and development. Mutant anthers fail to develop tapetum layer and produce excess numbers of microsporocytes while the other three somatic cell layers are unaffected. As a result, *ems1* mutants are male sterile since they are not able to produce any viable pollen. However, except for the anther phenotype, vegetative growth of the mutants is not affected.

The *Arabidopsis* *EXCESS MICROSPOROCTES1 (EMS1/EXS1)* gene encodes an LRR-RLK 1192 amino acids in length (Zhao et al., 2002; Canales et al., 2002). EMS1 shows structure of a typical *Arabidopsis* LRR-RLK, which includes an N-terminal extracellular domain with 30 LRRs as a potential interacting region for ligand binding or association with other proteins, a transmembrane domain which anchors the protein to the

cell membrane, and a cytoplasmic kinase domain responsible for phosphorylation modifications.

EMS1 belongs to the subfamily X of *Arabidopsis* LRR-RLKs (Shiu et al., 2001), together with BRI1 and FLS2, both of which work with co-receptors from the SERK family (Chinchilla et al., 2007; Li et al., 2002). In *Arabidopsis*, *EMS1* expression is detected in microsporocytes and tapetal cells of young floral buds, as well as in developing seeds.

The anther phenotype of *ems1* is also found in *tpd1* mutant anthers, which lack tapetum and the produce excessive microsporocytes. The *Arabidopsis* *TAPETUM DETERMINANT1* (*TPD1*) gene encodes a small protein consisting of 176 amino acids (Yang et al., 2003). The expression pattern of *TPD1* also coincides with *EMS1* in *Arabidopsis* anthers. However, unlike *EMS1*, *TPD1* expression is also detected in some other organs undergoing active cell division and differentiation, such as inflorescence meristems, floral meristems and carpel primordia.

Overexpression of *TPD1* alters cell fates in both carpel and anther, where cell divisions are promoted. The *TPD1* overexpression phenotype is dependent on the function of *EMS1* and the interaction of these two genes is not at the transcription level, which indicates that the TPD1 protein may physically interact with EMS1, possibly as its ligand (Yang et al., 2005). The potential interaction between EMS1 and TPD1 was confirmed by a recent study (Jia et al., 2008). The interaction was supported by three

lines of evidence: yeast two hybrid assays, GST pull-down assays, and coimmunoprecipitation experiments *in planta*.

1.1g SERK1 and SERK2 are involved in the regulation of *Arabidopsis* anther cell differentiation, possibly together with EMS1.

The *Arabidopsis* SERK protein family, which includes five members, falls within subfamily II of *Arabidopsis* LRR-RLKs (Shiu et al., 2001). Each SERK protein contains a relatively short LRR extracellular domain with only five LRRs. Members of the SERK protein family have been identified as interacting proteins of other LRR-RLKs from subfamily X in multiple *Arabidopsis* signaling pathways, such as plant hormone perception (Nam et al., 2002; Li et al., 2002), pathogen defense (Chinchilla et al., 2007) and cell-death regulation (He et al., 2007; Kemmerling et al., 2007). The redundancy shared among different SERK proteins was also noted in previous studies, during which multiple SERK proteins were found to work as co-receptors of a mutual LRR-RLK main receptor (Albrecht et al., 2008).

The SERK1 and SERK2 proteins have been reported to be important regulators during *Arabidopsis* anther cell differentiation and development (Albrecht et al., 2005; Colcombet et al., 2005). The *serk1 serk2* double mutants show a similar phenotype as both *ems1* and *tpd1* mutant plants, while neither *serk1* nor *serk2* single mutant shows any notable anther defects, which suggests functional redundancy between the *SERK1* and *SERK2* genes. Based on this indirect genetic evidence, a model has been proposed in

which SERK1 and SERK2 are redundant interacting proteins of EMS1 (Albrecht et al., 2008).

1.2 Research Objectives

Our central hypothesis for this study is that SERK1 SERK2 are co-receptors of EMS1, forming a protein complex that transmits signals to downstream effectors during anther development. The working model of the EMS1 protein complex in *Arabidopsis* anthers is described in Fig1.2.

In order to test our hypothesis and accomplish the overall objectives of this study, we propose the following three specific research objectives.

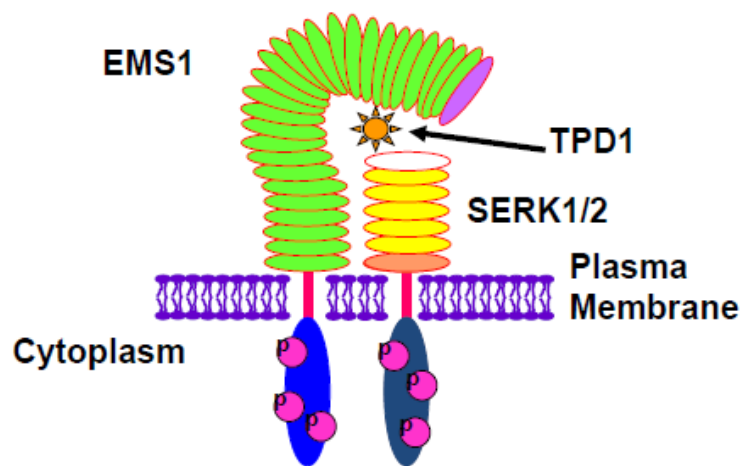


Fig1.2. Proposed working model of the EMS1 protein complex in *Arabidopsis* anthers.

Specific Objective 1: Determine the genetic interactions between *EMS1* and *SERK1/2*. Based on our preliminary data from genetic studies, our working hypothesis is that both *SERK1* and *SERK2* genetically interact with *EMS1*. *SERK1* and *SERK2* also share functional redundancy with each other during regulation of anther development.

Specific Objective 2: Determine the extent to which *SERK1/2* biochemically interact with *EMS1*. Our current working hypothesis, supported by preliminary data from the BiFC experiments, is that *SERK1* can physically interact with *EMS1* *in planta*. *SERK2* may also have physical interaction with *EMS1*. We plan to identify the functional domains which contribute to the interaction between *EMS1* and *SERK1/2*. BiFC and co-immunoprecipitation methods will be used to examine the interaction between *EMS1* and *SERK1/2*.

Specific Objective 3: Determine the biological significance of the interaction between *EMS1* and *SERK1/2*. Based on our preliminary data and previous studies by other researchers, our working hypothesis is that the association between *EMS1* and *SERK1/2* will lead to increased levels of phosphorylation on both interacting protein partners. The kinase activities of both *EMS1* and *SERK1/2* may also affect the formation and the function of the signaling complex. Phosphorylation on specific serine/threonine residues in the *EMS1* kinase domain is likely required for certain physiological functions in *Arabidopsis*. We plan to first identify *in vitro* phosphorylated residues within the

kinase domain of EMS1 and then further examine their significance using both *in vivo* and *in vitro* methods.

We expect to determine the exact roles of SERK1 and SERK2 in the EMS1 signaling pathway for the first time, based on evidence from both genetic and biochemical studies proposed in specific objectives 1 and 2. We also expect to provide details to better elucidate the working mechanism of the EMS1-SERK1/2 protein complex and its biological significance by evaluating the importance of both ligand binding and kinase activity of its protein components from the work proposed in specific objective 3.

Chapter 2: Materials and Methods

2.1 Strains, plasmids, primers and chemicals.

2.1.1 Strains: storage, cultures and transformation

The *E.coli* and *Agrobacterium tumefaciens* strains used in this study are listed in table 2.1. All strains were stored at -80 °C in 15% glycerol. For all liquid strain cultures, LB medium was used. For strain recovery from storage or transformation, 1.5% LB agar plates with specific antibiotics were used. *E.coli* strains were grown at 37 °C, except during induction for protein expression purpose, when they were grown at 16 °C. *Agrobacterium tumefaciens* strains were grown at 30 °C. Antibiotics were used for selection at the following concentrations: Kan, 50 µg/ml; Amp, 100 µg/ml; HmB, 50 µg/ml.

Table 2.1 *E.coli* and *Agrobacterium tumefaciens* strains used in this study

<u>Strains</u>	<u>Characteristics</u>	<u>Reference or source</u>
<i>E.coli</i>		
TOP 10	high-efficiency transformation	Invitrogen
BL21 (DE3)	protein express host strain	Novagen
<i>Agrobacterium tumefaciens</i>		
GV3101	for plant transformation	

2.1.2 Plasmids and primers.

Plasmids used or generated in this study are listed in table 2.2. Primers used in this study are listed in table 2.3.

Table 2.2 Plasmids used in this study

<u>Plasmids</u>	<u>Characteristics</u>	<u>Reference or source</u>
Original Plasmids		
pENTR-TOPO	cloning vector, for TOPO cloning and LR reaction with binary vector	Invitrogen
pET-28a	protein expression (with His tag)	Novagen
pGEX-4T-2	protein expression (with GST tag)	GE life sciences
pGWB1	binary vector, for cloning and plant expression	Nakagawa et al., 2007
pGWB16	binary vector, for cloning and plant expression	Nakagawa et al., 2007
pEarleyGate-301	binary vector, for cloning and plant expression, HA tag	Earley et al., 2006
pEarleyGate-302	binary vector, for cloning and plant expression, Flag tag	Earley et al., 2006
pSAT4-nEYFP-N1	BiFC vector, transient expression in <i>Arabidopsis</i> protoplasts	Tzfira et al., 2005
pSAT4-cEYFP-N1	BiFC vector, transient expression in <i>Arabidopsis</i> protoplasts	Tzfira et al., 2005
pSAT4-nEYFP-C1	BiFC vector, transient expression in <i>Arabidopsis</i> protoplasts	Tzfira et al., 2005
pSAT1-cEYFP-C1	BiFC vector, transient expression in <i>Arabidopsis</i> protoplasts	Tzfira et al., 2005

<u>Plasmids</u>	<u>Characteristics</u>	<u>Reference or source</u>
pSAT6-EYFP-N1	for marker gene fusion, transient expression in <i>Arabidopsis</i> protoplasts	Tzfira et al., 2005
Plasmids generated in this study		
For protein expression in <i>Arabidopsis</i>		
<i>SERK1::SERK2</i>	in pGWB1	this study
<i>SERK2::SERK1</i>	in pGWB1	this study
<i>SERK2::SERK2</i>	in pGWB1	this study
<i>EMS1::EMS1-cMyc</i>	in pGWB16	Jia et al 2008
<i>SERK1::SERK1-HA</i>	in pEarleyGate-301	this study
<i>SERK1::SERK1-FLAG</i>	in pEarleyGate-302	this study
<i>SERK1::SERK1-YFP</i>	in pEarleyGate-301	this study
<i>EMS1::EMS1 (T854A)</i>	in pGWB2	this study
<i>EMS1::EMS1 (S869A)</i>	in pGWB2	this study
<i>EMS1::EMS1 (S883A)</i>	in pGWB2	this study
<i>EMS1::EMS1 (S892A)</i>	in pGWB2	this study
<i>EMS1::EMS1 (T914A)</i>	in pGWB2	this study
<i>EMS1::EMS1 (S918A)</i>	in pGWB2	this study
<i>EMS1::EMS1 (T930A)</i>	in pGWB2	this study

<u>Plasmids</u>	<u>Characteristics</u>	<u>Reference or source</u>
<i>EMS1::EMS1</i> (T941A)	in pGWB2	this study
<i>EMS1::EMS1</i> (S1069A)	in pGWB2	this study
<i>EMS1::EMS1</i> (S1076A)	in pGWB2	this study
<i>EMS1::EMS1</i> (T1077A)	in pGWB2	this study
<i>EMS1::EMS1</i> (S1160A)	in pGWB2	this study
For recombinant protein expression in <i>E.coli</i>		
His-SERK1-KD	in pET-28a	this study
His-SERK1-KD (K330E)	in pET-28a	this study
His-SERK1-KD (S562A)	in pET-28a	this study
GST-EMS1-KD	in pGEX-4T-2	this study
GST-EMS1-KD (K945E)	in pGEX-4T-2	this study
GST-EMS1-KD (S1069A)	in pGEX-4T-2	this study
GST-EMS1-KD (S1073A)	in pGEX-4T-2	this study
GST-EMS1-KD (S1076A)	in pGEX-4T-2	this study
GST-EMS1-KD (S1077A)	in pGEX-4T-2	this study
GST-EMS1-KD (S1083A)	in pGEX-4T-2	this study

<u>Plasmids</u>	<u>Characteristics</u>	<u>Reference or source</u>
For fusion protein expression in <i>Arabidopsis</i> protoplasts		
cEYFP-EMS1	pSAT1-cEYFP-C1	this study
nEYFP-SERK1	pSAT4-nEYFP-C1	this study
EMS1-cEYFP	pSAT4-cEYFP-N1	this study
SERK1-nEYFP	pSAT4-nEYFP-N1	this study
BAK1-nEYFP	pSAT4-nEYFP-N1	this study
nEYFP-BAK1	pSAT4-nEYFP-C1	this study
cEYFP-EMS1-LRR-EMS1-TM	pSAT1-cEYFP-C1	this study
cEYFP-EMS-TM-EMS1-KD	pSAT1-cEYFP-C1	this study
nEYFP-SERK1-LRR-SERK1-TM	pSAT4-nEYFP-C1	this study
nEYFP-SERK1-TM-SERK1-KD	pSAT4-nEYFP-C1	this study
SERK1-cEYFP	pSAT4-cEYFP-N1	this study
EMS1-nEYFP	pSAT4-nEYFP-N1	this study

Table2.3 Primers used in this study

<u>Primer</u>	<u>Sequences (5'-3')</u>	<u>Application</u>
ZP817	CACCGCCGGCATGGCGTTTCTTAC	EMS1 F for TOPO cloning
ZP818	CGCTCGAGGTACCGGCTCATATCTCC	EMS1 R for TOPO cloning
ZP863	CTGCCGCGGTTACGAGACTTCAAATGGC	SERK1 Promoter F

Primer	Sequences (5'-3')	Application
ZP864	CGTGTCGACTTCAAACAACAATGCTAAATTTCCG	SERK1 Promoter R
ZP865	CTGCCGCGGCAAGAGGCGTGTATGGTTATGG	SERK2 Promoter F
ZP866	CGTGTCGACTTACCAAAAAAAAAAGCAAATTTCTCC	SERK2 Promoter R
ZP916	CACCGTCGACATGGAGTCGAGTTATGTGGTGT	SERK1 F
ZP917	CCTTGGACCAGATAACTCAACG	SERK1 R w/o stop
ZP918	CACCATGGGGAGAAAAAAGTTTGAAGC	SERK2 F
ZP919	TCTTGGACCAGACA ACTCCATAG	SERK2 R w/o stop
ZP819	CACCGGATCCCGCAGATGGGCTAT	EMS1KD F for TOPO cloning
ZP2086	CAGGATCCTTCCAAGGCATTGCTTTC	for EMS1 mutated version cloning
ZP 2103	TTGGGCGCGCCATGGTCCGACTCAG	YFP F for SERK1-YFP
ZP 2104	CGGGCGCGCCCTAGGTGGATCTTCAC	YFP R for SERK1-YFP
Plant genotyping primers		
OMC 489	CCGTTTACCGTTTTGTATATCCCG	DS5-1 for <i>ems1</i>
OMC 499	AACAAACCCCGTCAGCTTTA	EMS1 pf-407 for <i>ems1</i>
OMC500	ACCGGAGAAGTGGTTGTCAC	EMS1 cr453 for <i>ems1</i>
ZP786	ACAACGCTTTACAGCAAGAACGGAAT	SAIL T-DNA Left border primer
ZP792	ATTTTGCCGATTCGGAAC	SALK T-DNA Left border primer 1.3

Primer	Sequences (5'-3')	Application
ZP554	AGTGAAGAGCGAGAAGGAACC	SALK_058020 LP (SERK2)
ZP555	AAGGCTTAGGCTTTTGTGG	SALK_058020 RP (SERK2)
ZP556	ATACACAAAAGTGAAACGGCG	SALK_044330 LP (SERK1)
ZP557	TAATGACACAGAGAGGCCACC	SALK_044330 RP (SERK1)
ZP863	CTGCCGCGTTACGAGACTTCAAATGGC	SALK_080572 RP (SERK1)
ZP864	CGTGTCGACTTCAAACAACAATGCTAAATTTC G	SALK_080572 LP (SERK1)
ZP866	CACCGTCGACATGGCGTTTCTTACCGCATT	CS_821736 RP/ SALK_025016 RP- 1 (SERK2)
ZP1855	GCAGTATACTGCGGGTTAAAATC	CS_821736 RP SALK_025016 RP- 2 (SERK2)
ZP1856	GAGGAAATACTTACCAAACAAATC	CS_821736 LP SALK_025016 LP (SERK2)
SERK1/2 cloning and mutagenesis primers for protein purification in <i>E.coli</i>		
ZP1919	TCCCATATGATTTTCTTCGATGT	SERK1 KD F for pET-28a
ZP1920	ATAAAGCTTTTACCTTGGACCAG	SERK1 KD R for pET-28a
ZP1921	AATCATATGGACCCTGAGGTTCA	SERK2 KD F for pET-28a
ZP1922	CCGAAGCTTTTATCTTGGACCAG	SERK2 KD R for pET-28a

Primer	Sequences (5'-3')	Application
ZP1960	TGTTGCTGTCGAGAGACTGAAGG	mSERK1 K330E F
ZP1961	CCTTCAGTCTCTCGACAGCAACA	mSERK1 K330E R
ZP2017	CACGCAAGGAGCACCAATGGAAAG	mSERK1 S562A F
ZP2018	CTTTCCATTGGTGCTCCTTGCGTG	mSERK1 S562A R
BiFC primers		
ZP2010	CATCCGGAATGGAGTCGAGTTATGT	cEYFP-SERK1 F
ZP2011	GCGTCGACTTACCTTGGACCAGATA	cEYFP-SERK1 R
ZP2012	AGCCATGGTCATGGAGTCGAGTTATG	SERK1-cEYFP F
ZP2013	GCGGTACCGCCTTGGACCAGATAACT	SERK1-cEYFP R
ZP1108	CACCCCATGGTCGAGTCGAGTTATGTGGTG	SERK1-nEYFP F
ZP1109	ACCGTCGACTCCTTGGACCAGATAACTCAAC	SERK1-nEYFP R
ZP1110	CACCGTCGACATGGAGTCGAGTTATGTGGTG	nEYFP-SERK1 F
ZP1111	GGCCCGCGGTTACCTTGGACCAGATAACTCAAC	nEYFP-SERK1 R
ZP1258	CACCCTCGAGCATGGAACGAAGATTA	BAK1-nEYFP F
ZP1259	GCGGTACCGTCTTGGACCCGAGGGG	BAK1-nEYFP R
ZP1260	CACCCTCGAGCTATGGAACGAAGATT	nEYFP-BAK1 F
Zp1261	GCGGTACCTTATCTTGGACCCGAGG	nEYFP-BAK1 R
ZP802	GATCTCGAGCATGGCGTTTCTTACCGCATTGTT	EMS1-nEYFP & EMS1-cEYFP F
ZP804	GCGGTACCGTATCTCCTTAAGAGCCTTCAAC	EMS1-nEYFP & EMS1-cEYFP R
ZP803	GATCTCGAGCTGATCTTAGCTCGGAAACAAC	EMS1 cf64
ZP1041	CAGGTACCATGATCTGTAGCCTCGACAATATC	EMS1 cr2748
ZP2113	TAGCTGTTTGCCAACCGGTCAAC	For cloning SERK1 SP

<u>Primer</u>	<u>Sequences (5'-3')</u>	<u>Application</u>
ZP2114	GCCCATGGCATTAGCAGAAGCAAG	SERK1 signal peptide R (27 th aa)
ZP2115	CAGTCGACTTGGAAGGTGATGCTTT	F from SERK1 28 th aa
ZP2116	GCGGTACCTTAATCACTCGCCAC	SERK1 300 th aa with STOP
ZP2117	CAGTCGACGGCTCCTTCTCACTC	SERK1 F after 4 th LRR (from 185 th aa)
ZP2118	GCGGTACCTTACCTTGGACCAGA	R to SERK1 589 th aa with STOP
ZP2119	GACTCGAGCTGATCCTTCCAAGGCATTG	F EMS1 cf 2386
ZP2120	CGGGTACCTCATATCTCCTTAAGAGCCT	R EMS1 cr 3579
EMS1 mutagenesis primers		
ZP1966	CAGTAGCGGTGGAGAAGCTAAGTGA	K945E F
ZP1967	TCACTTAGCTTCTCCACCGCTACTG	K945E R
ZP 807	GCTAGCAAGACTAATTGCTGCCTGTGAATCCC	S1069A F
ZP 808	GGGATTCACAGGCAGCAATTAGTCTTGCTAGC	S1069A R
ZP 809	GTG CCT GTG AAGCCCATGTTAGTACAGTC	S1073A F
ZP 810	GAC TGT ACT AAC ATG GGC TTCACA GGC AC	S1073A R
ZP 811	GTGAATCCCATGTTGCTACAGTCATAGCAG GG	S1076A F
ZP 812	CCCTGCTATGACTGTAGCAACATGGGATTCAC	S1076A R
ZP 813	GAATCCCATGTTAGTGCCGTCATAGCAGGGAC	T1077A F
ZP 814	GTCCCTGCTATGACGGCACTAACATGGGATTC	T1077A R
ZP 815	CAGTCATAGCAGGGGCTTTCGGGTATATCCC	T1082A F

<u>Primer</u>	<u>Sequences (5'-3')</u>	<u>Application</u>
ZP 816	GGGATATACCCGAAAGCCCCTGCTATGACTG	T1082A R
ZP1996	AGATGGGCTATGGCAAAGAGAGTGAAG	T854A F
ZP1997	CTTCACTCTCTTTGCCATAGCCCATCT	T854A R
ZP1998	CGAATGGAGGAAGCCAGATTGAAAGGG	S869A F
ZP1999	CCCTTTCAATCTGGCTTCCTCCATTCG	S869A R
ZP2000	AGGGAGCCTTTAGCCATCAATATAGCA	S892A F
ZP2001	TGCTATATTGATGGCTAAAGGCTCCCT	S892A R
ZP2002	ACAGATCATTTTCGCTAAGAAGAACATT	S918A F
ZP2003	AATGTTCTTCTTAGCGAAATGATCTGT	S918A R
ZP2004	CCAGGTGAGAAAGCAGTAGCGGTGAAG	T941A F
ZP2005	CTTCACCGCTACTGCTTTCTCACCTGG	T941A R
ZP2105	CTGTATTTCTTAGCTGGAAGCAGATCA	S883A F
ZP2106	TGATCTGCTTCCAGCTAAGAAATACAG	S883A R
ZP2107	ATTGTCGAGGCTGCAGATCATTTCTCT	T914A F
ZP2108	AGAGAAATGATCTGCAGCCTCGACAAT	T914A R
ZP2109	GGTGGTTTTGGGGCGGTTTACAAAGCT	T930A F
ZP2110	AGCTTTGTAAACCGCCCCAAAACCACC	T930A R
ZP2111	GCTTTGAAGAACGCTCAGCTTCGTCTG	S1160A F
ZP2112	CAGACGAAGCTGAGCGTTCTTCAAAGC	S1160A R

2.2 Genetic Studies

2.2a Plant materials and growth conditions

In this study, all *Arabidopsis* plants were grown at 23 °C under a photoperiod of 16 hours light and 8 hours dark in Metro-Mix 360 soil (Sun-Gro Horticulture). The wild type plants used are *Arabidopsis* ecotype Columbia (Col) plants. Ds and T-DNA insertion lines used in this study are summarized in Fig 2.1. Among these lines, three lines were previously reported, *serk1-1* (SALK_044330), *serk2-1* (SALK_058020) and *ems1* (Albrecht et al., 2005; Colcombet et al., 2005; Zhao et al., 2002).

Identification of new *ems1* and *serk1/2* T-DNA lines

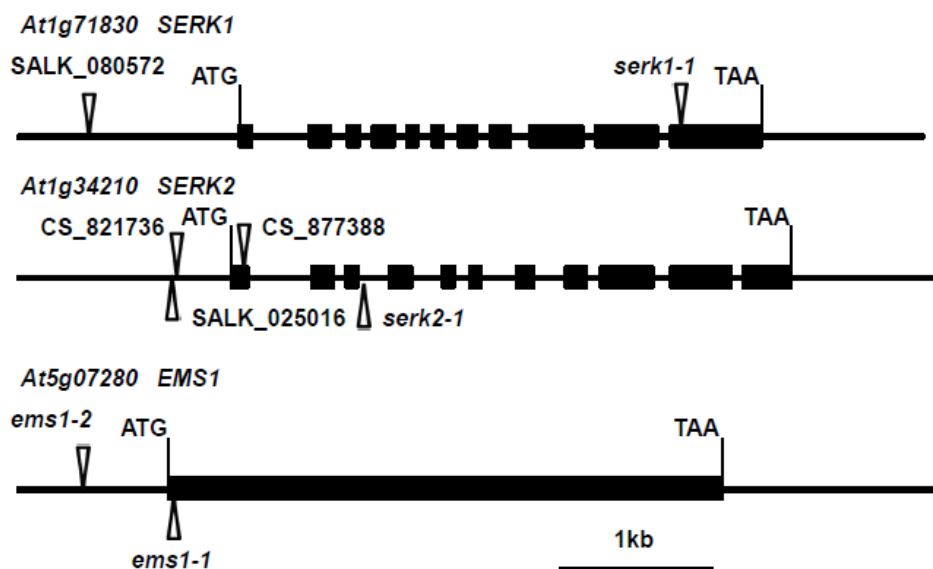


Fig 2.1 *Arabidopsis* insertion mutant lines identified and used in this study

Coding regions of *EMS1* and *SERK1/2* genes are indicated by black blocks while non-coding regions are represented by the black lines. Triangles reflect the positions for Ds or T-DNA insertions.

From the ABRC collection (Arabidopsis Biological Resource Center, Ohio State University, USA), five T-DNA lines were newly identified for *ems1* and *serk1/2*: SALK_080572 (*SERK1*, promoter); CS_821736 (*SERK2*, promoter); SALK_025016 (*SERK2*, promoter); CS_877388 (*SERK2*, 1st exon); SALK_051989 (*EMS1*, promoter, named as *ems1-2*). Most of these chosen lines have T-DNA insertions within promoter regions which are very likely to partially reduce gene expression generate weak alleles for the genetic studies.

RT-PCR examination of gene expression in *ems1-2* line

Young inflorescences from Col-0 and *ems1-2* plants were collected right immediately before flowering for total RNA extraction. 60 to 100 mg of plant materials was used. Total RNA extraction was performed using an RNeasy Plant mini kit from QIAGEN (CA, USA).

For RT-PCR, cDNA templates were first generated separately from 1 µg of total RNAs from Col-0 or *ems1-2*, using a QuantiTect Reverse transcription kit from QIAGEN (CA, USA). For RT-PCR, *ACTIN2* was used as an internal control. 28 cycles were used for *EMS1* expansion, while 22 cycles were used for *ACTIN2* comparison.

Genotyping of *Arabidopsis* T-DNA and Ds lines

Plant genomic DNA extraction

For genomic DNA extraction from *Arabidopsis* plants, leaves were cut and placed into 1.5mL microcentrifuge tubes after plants and corresponding tubes were numbered. Samples were placed on dry ice for 3 minutes to facilitate grinding. 150µl of Edward's buffer (200mM Tris pH7.5, 250mM NaCl, 25mM EDTA, 0.5% SDS) was added to each tube before grinding with plastic pestles. In the next step, 150µl of phenol: chloroform: isoamyl alcohol mixture (25:24:1 saturated with 10mM Tris, pH 8.0, 1mM EDTA) was added to each tube and mixed well by vortexing. Samples were then centrifuged at 12000 rpm for 10 minutes. 120µl supernatant was then transferred from each tube to a new tube containing 240µl of ice cold 100% ethanol. After mixing, samples were centrifuged again at 12000 rpm for 10 minutes. Precipitated plant genomic DNA samples were washed with 70% ethanol and then air dried. Plant genomic DNA samples were stored at -20 °C after adding 40µl of distilled water to each tube.

PCR examination of genetic background

For PCR reactions, 1 µl of prepared genomic DNA was used. 0.3 µl of Taq DNA polymerase was used for each reaction, using 1minute/kb for extension and 30 cycles for the whole amplification.

Samples from homozygous plants yielded product bands only when the Left Border + Right Primer pair was used. Samples from heterozygous plants yielded products

when using either Left Border + Right Primer pair or Left Primer + Right Primer pair. For initial identification from original seed stocks, Left Border + Right Primer pair was first used to detect the presence of T-DNA. For identified homozygous lines, Left Primer + Right Primer pair was used first to reconfirm their genetic background.

Generation of *Arabidopsis* double/triple mutant lines

Crosses of *Arabidopsis* plants

Unopened young *Arabidopsis* flower buds were chosen for sterilization from one of the two parent lines. Sepals, petals and stamens were carefully removed using tweezers, leaving only the unfertilized gynoecia. After 24 hours, pollen from the other parent line was applied to surviving gynoecia after sterilization. Individual branches were then labeled with tape to record information of both lines used for the crosses. Siliques elongated a few days after successful manual pollen application. Seeds were harvested 2-3 weeks later, after siliques turned completely yellow.

Double/triple *Arabidopsis* mutant line generation

The following double and triple *Arabidopsis* mutant lines were generated by crossing. Homozygous lines were also identified from F2 or F3 populations, except for lines which were completely sterile.

ems1-2 serk1-1

ems1-2 serk2-1

ems1-2 CS_877388

serk1-1 CS_877388 (sterile)

serk1-1 serk2-1 (sterile)

serk1-1 CS_821736

serk1-1 SALK_025016

SALK_080572 CS_877388

SALK_080572 *serk2-1*

ems1-1 serk1-1 serk2-1(sterile)

AtML1::TPD1 / serk1-1 serk2-1(sterile)

2.2b Phenotypic analysis

Plant fertility loss evaluation

To evaluate plant fertility, 30 individual plants were chosen from each different genetic background to examine and count siliques. The first 20 siliques produced on main branch of the plants were examined for fertility evaluation. Based on the length of each

silique, they were recorded as sterile, semi-sterile or fertile. For the record, every five siliques were then grouped based on their positions into four categories.

Pollen staining examination

Young *Arabidopsis* inflorescences with undehisced anthers were collected and fixed in Östergren & Heneen's fixative (1962) for 24 hours. Samples were then rehydrated in a graded series as follows: 70%, 50%, 30% ethanol and distilled water. Samples were kept for 30 minutes in each dilution. After removing excess water with paper towels, samples were put into staining buffer and incubated at 50 °C for 24-48 hours before light microscopy observation.

2.2c Semi-thin section analysis of *Arabidopsis* inflorescences

Fixation, post-fixation, dehydration and resin infiltration

Entire young *Arabidopsis* inflorescences were cut from plants and put into fixation buffer (2.5% glutaraldehyde in 0.1 M HEPES buffer, with 0.02% Triton X-100) at room temperature for overnight fixation. Three 15 min washes were then performed in 0.1 M HEPES buffer (with 0.02% Triton X-100).

Post-fixation was done in 1% OsO₄ (in distilled water) in the dark for overnight at room temperature. Afterwards, samples were washed in distilled water three times, 15 minutes for each wash.

Dehydration was performed in a graded series of acetone, starting with 10% acetone, with 10% concentration increase each time, ending up in 100% acetone. Two additional incubations in fresh 100% acetone were also performed. Incubation time was 90 minutes in every concentration.

For infiltration using Spurr's resin, 100% resin was first prepared according to the manufacturer's recipe for direct use or acetone dilution. Resin infiltration was started in 20% Spurr's resin (in acetone), with 20% concentration increase each time, ending up in 100% Spurr's resin. Infiltration time was 3 hours in every concentration. Two additional 24 hour infiltrations in fresh 100% Spurr's resin were also performed.

Sample dissection and emdedding

Buds from inflorescence samples were dissected in 100% Spurr's resin under a dissection microscope and orientated in freshly prepared 100% Spurr's resin in silicone rubber molds. Molds with embedded sample buds were then labeled with sample information and put into 60 °C oven for overnight resin polymerization.

Semi-thin sectioning

Individual *Arabidopsis* bud sample resin blocks were first trimmed using razor blades under dissection microscope and then mounted onto an RMC MT 7000 ultramicrotome. Sectioning was done using glass knives. Sections at about 0.5 μ m thickness were cut and floated on water in the boat glued on the glass knife. Sections were carefully collected and transferred to distilled water droplets on a glass slide surface and then dried on a hot plate. After drying the water, markers were used to label the slide with resin block information and circle section locations on the slide. A few drops of 1% toluidine blue staining solution was used to cover sections on the slide before putting the slide back on the hot plate. Slide was removed from the hot plate and rinsed using running tap water when the edge of the stain drops showed a golden color. Excessive water was again removed using a hot plate. The sections were then observed and photographed with an Olympus BX51 microscope and Olympus DP70 digital camera for quality examination and anther cell development analysis.

2.2d *Arabidopsis* plant transformation

For each transformation, a single colony from an appropriate *Agrobacterium tumefaciens* strain was used for the initial small scale culture in 5ml of LB medium with antibiotics at 30 °C. After 24 hours, 2-3 ml from the small culture was used for inoculation of a 200-300 ml expanded overnight culture. Cells were then collected by centrifuging at 6500 rpm for 5 minutes, and resuspended in 200 ml of 5% sucrose

solution (with 0.02% Silwet L-70) before being used for plant transformation. Plant transformation was done by either spray or dipping method (Clough et al., 1998). For plants in Col-0 background, dipping method was efficient enough to generate sufficient numbers of transformants. For plants in *Ler* background, spray method is essential in order to obtain a acceptable transformation efficiency.

2.2e *Arabidopsis* transformant analysis

Seeds from transformed *Arabidopsis* plants were harvested and then dried using silicon desiccant before being screened either in soil by herbicides Basta spray or on ½ MS media plates with antibiotics. In the situation in which initial transformant screenings were performed on ½ MS media plates with antibiotics, transformants were transferred to soil after becoming distinguished from other seedlings carrying no transgenes.

2.3 Biochemical studies.

2.3a Examination of EMS1 and SERK1 interaction using BiFC

Bimolecular fluorescent complementation (BiFC) technique has been widely used to examine the interaction between proteins and protein subcellular localizations in living plant cells (Ohad et al., 2007; Walter et al., 2004). During BiFC assays, the interested protein pairs are fused with each half of the YFP or other GFP variant protein

and then co-expressed in living plant cells. The reconstitution of YFP or other GFP variant protein occurs when the tested protein pairs can interact with each other. The fluorescence signal from reconstituted proteins can be observed by confocal microscopy.

Plasmid construction and preparation for BiFC

For full length protein expression in *Arabidopsis*, EMS1, SERK1 and BAK1 were amplified using either BAC or cDNA templates. Constructs were generated for testing the following pairs of fusion proteins:

EMS1-cEYFP + SERK1-nEYFP

EMS1-cEYFP + BAK1-nEYFP (negative control)

cEYFP-EMS1 + nEYFP-SERK1

cEYFP-EMS1 + nEYFP-BAK1 (negative control)

EMS1-cEYFP + EMS1-nEYFP

SERK1-cEYFP + SERK1-nEYFP

For making truncated versions of EMS1 and SERK1 in order to probe the potential functional interacting domains, a short signal peptide sequence from either *EMS1* or *SERK1* was first cloned into BiFC vectors separately, fusing right after either half of the EYFP. Partial coding sequences of EMS1 or SERK1 were then fused to the C terminal of either half EYFP, yielding these two testing pairs:

cEYFP-EMS1-LRR-EMS1-TM + nEYFP-SERK1-LRR-SERK1-TM

cEYFP-EMS1-TM-EMS1-KD + nEYFP-SERK1-TM-SERK1-KD

For high quality plasmid preparation, PureYield plasmid miniprep/midiprep systems (Promega, Madison, WI, USA) were used to isolate plasmid DNAs for *Arabidopsis* protoplast transfection. In order to obtain a high yield of plasmid DNA, 6 to 8 ml overnight *E.coli* cultures were used for each preparation.

Preparation of *Arabidopsis* protoplasts

Rosette leaves from young *Arabidopsis* wild type or *tpd1* plants (3-4 weeks old) were used for preparation of protoplasts. After collecting leaves from plants, 3M Magic Tape was used to remove the lower epidermal cells to expose mesophyll cells. For following enzyme digestion, 7-10 peeled leaves were digested in a Petri dish containing 10 ml of enzyme solution (1% cellulose R10 (Yakult, Tokyo, Japan), 0.25% macerozyme R10 (Yakult, Tokyo, Japan), 0.4 M mannitol, 10 mM CaCl₂, 20 mM KCl, 20 mM MES, pH 5.7, 10 mM CaCl₂ and 0.1% BSA). Drops of the digestion solution were checked by light microscopy after the solution color turned green, which was an indication of successful digestion. Total digestion time was limited to a maximum of 4 hours.

Enzyme solution containing protoplasts was filtered through 35 μm nylon mesh and centrifuged at 100 g in 50 ml centrifuge tubes for 2 minutes to pellet protoplasts. Protoplasts were then resuspended and washed twice in ice cold W5 wash solution

(154mM NaCl, 125mM CaCl₂, 5mM KCl and 2mM MES, pH 5.7). Washed protoplasts were resuspended in MMg solution (0.6M mannitol, 15mM MgCl₂ and 4mM MES, pH 5.7) before PEG transfection.

Transfection of *Arabidopsis* protoplasts

For each transfection, 10 µl of plasmid DNA (10-20µg) was first added to a 1.5 ml microcentrifuge tube. 100 µl of protoplast solution was then added and mixed well. An equal volume (110 µl) of PEG/CaCl₂ solution (40%, 4g PEG 4000 (Fluka,#81240), 3ml H₂O, 2.5ml 0.8M mannitol, 1ml 1M CaCl₂) was then added to the tube and mixed well. The tube was then incubated at 23 °C for 30 minutes.

After incubation, 440 µl of W5 solution was added to the tube to stop transfection by diluting the mixture by mixing. The resulting solution was centrifuged at 100 g for 2 minutes to pellet protoplasts and remove PEG. Protoplasts were then gently resuspended and diluted in 100 µl of W5 solution. More W5 solution was carefully added, making the final volume 1ml. The tube was then wrapped in foil and left at 4 °C overnight before analyzed by confocal microscopy.

2.3b Preparation for co-immunoprecipitation examination of EMS1 and SERK1 in *Arabidopsis* anthers

Plasmid construction for SERK1 protein expression in *Arabidopsis*

The *SERK1* promoter and full length cDNA were amplified with PCR and separately cloned into pENTR-TOPO vectors. Both were then digested with SacII and Sall and gel purified for ligation. The SERK1::SERK1 was introduced into pEarleyGate-301 (HA tag) and pEarleyGate-302 (Flag tag) via LR clonase reaction, which led to a recombination between the pENTR-TOPO vector and the binary vector.

For making one additional SERK1::SERK1-YFP construct, YFP was PCR amplified with Phusion high fidelity DNA polymerase (NEB, MA, USA) and the pSAT6-EYFP-N1 vector as template. The product was then gel purified after AscI digestion. SERK1::SERK1 in pENTR-TOPO was also digested with AscI and then gel purified. Both purification products were analyzed in 1% agarose gels before used for ligation.

For heat shock transformation, 2 μ l of ligation product was used. Single colonies were picked from LB+ Kan plate for overnight culture and plasmid isolation. Plasmids were examined by PCR using cloning primers (ZP2103+ZP2104). Plasmid DNA was extracted from positive clones for introduction into the binary vector pEarleyGate-302, via LR clonase reaction.

SERK1 transformant generation and screening

Plant transformation was performed separately using *Agrobacterium tumefaciens* strains containing one of the three kinds of tagged SERK1::SERK1 binary vector as described previously. Transformants were obtained by herbicides Basta spray screening in soil. Transformants were kept and labeled. Genomic DNAs were also isolated from transformants for PCR examination to confirm the presence of T-DNA in each individual plant.

Generation of *EMS1:: EMS1-cMyc/ ems1-2 serk1-1* plants

The construct of *EMS1:: EMS1-cMyc* was initially generated and used for co-immunoprecipitation purpose in a recent study from our lab (Jia et al.,2008). In this study, we also introduced *EMS1:: EMS1-cMyc* into the *ems1-2 serk1-1* background, which rescued the reduced fertility phenotype, as expected.

2.4 Phosphorylation analysis of EMS1

2.4a Identification of *in vitro* phosphorylation residues within the EMS1 kinase domain

Plasmids construction for GST-EMS1-KD fusion protein expression

The kinase domain of EMS1 (aa849-aa1192) was amplified with PCR using Phusion high fidelity DNA polymerase (NEB, MA, USA) from its BAC template and then digested with BamHI and XhoI before ligation into the pGEX-4T-2 expression

vector. For heat shock transformation, 2 μ l ligation product was used. Colonies yielded from overnight incubation on LB agar plates with Amp were cultured for plasmid DNA isolation. After confirmation by restriction enzyme digestion, the GST-EMS1-KD-pGEX-4T-2 plasmid was introduced into the BL21DE3 strain via electroporation.

GST-EMS1-KD recombinant protein expression and purification

An single colony was used for the initial small scale overnight culture in 5ml LB medium with Amp. The culture was then expanded to 100-200ml after adding 1-2ml from the overnight culture. OD600 was monitored every half hour until it reached 1.0 before IPTG was added. A final concentration of 0.5mM IPTG was used for protein induction at 16 °C for 16-18 hours on a 180 rpm shaker.

After induction, cells were collected by centrifuging at 6500 rpm at 4 °C for 5 minutes in 50ml centrifuge tubes and resuspended in 2-5 ml GST binding buffer (50 mM Tris-HCl, pH 7.4, 150 mM NaCl, 10 mM EDTA, 1 mM DTT, Lysozyme (0.75 mg/mL), 1 mM PMSF, DNase I 500u/ml, 10 mM 2-mercapatomethanol, 1% TWEEN 20 and 1% TRITON X-100). The mixture was incubated on ice for 20 minutes before being subjected to sonication on ice (12W, 3 second on/off cycles, 5-10 minutes total time). After sonication, the solution was first centrifuged at 9000 rpm at 4 °C for 15 minutes (in 50 ml centrifuge tubes). The supernatant was transferred to 1.5 ml microcentrifuge tubes and then centrifuged at 12000 rpm at 4 °C for 20 minutes. This was repeated for another 1 to 2 times until the crude protein solution was clear.

50-200 μ l of GST beads (GE Life Sciences, PA, USA) in 75% slurry was used to bind GST tagged protein from the previously prepared crude protein. The slurry was first transferred to a clean 1.5 ml microcentrifuge tube and centrifuged at 3600rpm at 4 $^{\circ}$ C for 5 minutes. After removing the supernatant, beads were resuspended and washed in ice cold PBS. Beads were then collected by centrifuging at 3600rpm at 4 $^{\circ}$ C for 5 minutes. The PBS was carefully removed using a pipette.

Crude protein solution was added to the tube and mixed well with the GST beads. Tubes were fixed with tape on a slow shaker for incubation at 4 $^{\circ}$ C for 1-2 hours. Incubation time could be extended up to 8 hours when a protease inhibitor cocktail pill (Pierce Biotechnology, IL, USA) was added.

GST beads were collected by centrifuging at 3600rpm at 4 $^{\circ}$ C for 5 minutes after incubation. GST wash buffer (50mM Tris-HCl, pH 7.4, 500mM NaCl, 10mM EDTA, 1mM DTT, 1mM PMSF, 10 mM 2-mercapatomethanol, 1% TWEEN 20 and 1% TRITON X-100) was used to wash the GST beads. Three 15 min washes were performed on a slow shaker at 4 $^{\circ}$ C. Wash buffer was completely removed after the final wash. With the addition of a protease inhibitor cocktail pill in the wash buffer, wash times could be increased to five times, if necessary.

GST-EMS1-KD protein was eluted using 5 volumes of GST elution buffer (50 mM Tris-HCl, pH 8.0, 20 mM glutathione). Up to three elutions were collected. Eluted proteins were quickly analyzed by SDS-PAGE, followed by *in vitro* autophosphorylation assay.

***In vitro* autophosphorylation assay of GST-EMS1-KD protein**

For *in vitro* autophosphorylation assay, the final concentration of GST-EMS1-KD recombinant protein was adjusted to 1-2 $\mu\text{g}/10\mu\text{l}$. Protein kinase buffer (10X) from NEB was used. Each reaction was incubated at 25 °C in 20 μl volume for 1 hour and terminated by adding 6X SDS-PAGE sample buffer. Samples were analyzed with SDS-PAGE. Stained bands of GST-EMS1-KD recombinant protein were cut from the gel and mailed to collaborators for further LC/MS/MS analysis of phosphorylated residues.

2.4b *In vitro* transphosphorylation between kinase domains of EMS1 and SERK1

Plasmid construction for His-SERK1-KD fusion protein expression

The kinase domain of SERK1 (aa270-aa625) was amplified with PCR using Phusion high fidelity DNA polymerase (NEB) from its BAC template and then digested with NdeI and HindIII before ligation into the pET-28a expression vector. Colonies yielded from overnight incubation on LB agar plates with Kan were cultured for plasmid DNA isolation. After restriction enzyme digestion confirmation, the His-SERK1-KD-pET-28a plasmid was introduced into BL21DE3 strain via electroporation.

His-SERK1-KD recombinant protein expression and purification

A single colony was used for the initial small scale overnight culture in 5ml of LB medium with Amp. The culture was then expanded to 50ml after adding 1-2ml from the overnight culture. OD600 was monitored every half hour until it reached 0.5 before addition of IPTG. A final concentration of 0.05mM IPTG was used for protein induction at 16 °C for 16-18hours.

After induction, cells were collected by centrifuging at 6500 rpm at 4 °C for 5 minutes in 50ml centrifuge tubes and resuspended in 2ml His binding buffer (50 mM Na₃PO₄, pH 8.0, 300mM NaCl, 10 mM imidazole, 1 mM DTT, Lysozyme (0.75 mg/ml), 1 mM PMSF, DNase I 500u/ml, 10mM 2-mercapatomethnol, 1% TWEEN 20,1% TRITON X-100). The mixture was incubated on ice for 20 minutes before being subjected to sonication on ice (12W, 3 seconds on/off, 10 minutes total). After sonication, the solution was first centrifuged at 9000 rpm at 4 °C for 15 minutes (in 50 ml centrifuge tubes). The supernatant was transferred to 1.5 ml microcentrifuge tubes and then centrifuged at 12000 rpm at 4 °C for 20 minutes. One or two more repeats were performed until the crude protein solution was clear.

20-30µl of HIS-Select Nickel Affinity Gel (Sigma, MO, USA) in 50% slurry was used for binding of His-SERK1-KD protein from previously prepared crude protein extracts. The slurry was first transferred to a clean 1.5 ml microcentrifuge tube and centrifuged at 6500 rpm at 4 °C for 5 minutes. After removing supernatant, beads were resuspended in His wash buffer (50 mM Na₃PO₄, pH 8.0, 300 mM NaCl and 20 mM imidazole) for washing. Beads were then collected by centrifuging at 6500rpm at 4 °C for 5 minutes.

Crude protein solution was added to the tube and mixed well with the HIS-Select Nickel Affinity Gel. Tubes were fixed with tape on a slow shaker for incubation at 4 °C for 1-2 hours. There was no need to use extended incubation time based on our experimental results of consistent high yield of his-SERK1-KD fusion protein.

HIS select nickel affinity gel was collected by centrifuging at 6500 rpm at 4 °C for 5 minutes after incubation ended. His wash buffer (50 mM Na₃PO₄, pH 8.0, 300 mM NaCl and 20 mM imidazole) was used to wash the gel. Three washes were performed on a slow shaker at 4 °C, 15 minutes for each. Wash buffer was completely removed after the final wash.

His-SERK1-KD protein was eluted using 5 volume of His elution buffer (50 mM Na₃PO₄, pH 8.0, 300 mM NaCl and 250 mM imidazole). Up to three washes were used. Elutes were quickly analyzed by SDS-PAGE followed by in vitro autophosphorylation assay. His-SERK1-KD protein consistently showed high concentration in elutes.

***In vitro* cross phosphorylation between His-SERK1-KD and GST-EMS1-KD recombinant protein**

Purified His-SERK1-KD and GST-EMS1-KD recombinant proteins according to the described methods were used to perform in vitro cross phosphorylation assays.

For in vitro cross phosphorylation assays, the final concentration of each kind of recombinant protein was adjusted to 1-2 µg/10 µl. Protein kinase buffer (10X) from NEB was used. For each reaction, 1 µl (10 µCi) γ-³³P labeled ATP was added. Each reaction

was incubated at 25 °C in 20 µl volume for 1 hour and terminated by adding 6X SDS-PAGE sample buffer.

In total, three phosphorylation assay groups were included, two auto phosphorylation assay groups of His-SERK1-KD and GST-EMS1-KD as controls, and a third group with co-incubation of His-SERK1-KD and GST-EMS1-KD.

After sample separation by SDS-PAGE, gels were kept on a plate which recorded the signal from γ -³³P labeled ATP in a Storage Phosphor Screen cassette overnight. On the following day, the plate was scanned on the Amersham Storm 860 imaging system (Amersham Biosciences Corp, NJ, USA) for filmless autoradiography imaging capture. The gel was then stained using the Coomassie brilliant blue staining method.

Mutagenesis of His-SERK1-KD and GST-EMS1-KD recombinant protein

Mutagenesis experiments were performed to generate kinase inactive His-SERK1-KD and GST-EMS1-KD recombinant proteins, in order to further examine the potential transphosphorylation between their active and inactive forms.

For the His-SERK1-KD, based on previous reports (Shah et al., 2001 and Karlova et al., 2009), mutations of S562A or K330E almost complete abolished autophosphorylation activity of SERK1. The overlapping PCR method was used for mutagenesis work to introduce the above two mutations separately into His-SERK1-KD. The two fragmented templates were generated in separate PCR reactions, each in 20 µl

volumes and then gel purified before being eluted in 100 μ l of distilled water. For the final cloning into the pET-28a expression vector, steps described previously were followed.

For GST-EMS1-KD, due to lack of information from previous studies, two approaches were tried to generate its inactive forms.

The first try was based on phylogenetic analysis and identification of conserved residues among *Arabidopsis* LRR-RLKs and experimental support from previous studies. We found residue K945 in EMS1 to be highly conserved among *Arabidopsis* LRR-RLKs. Moreover, mutations of corresponding residues in BRI1 (K911E), BAK1 (K317E) and SERK1(K330E) all abolished the autophosphorylation activities of the proteins (Oh et al., 2000, Shah et al., 2001 and Wang et al., 2008) Based on this supporting evidence, the K945E mutation was introduced into GST-EMS1-KD using the previously described method.

The second effort was to introduce mutations to serine/threonine residues within the activation loop of GST-EMS1-KD. Five mutated versions of GST-EMS1-KD were generated: S1069A, S1073A, S1076A, T1077A and T1083A. According to the general working mechanisms of LRR-RLKs, one or two serine/ threonine residues within the activation loop are essential to maintain autophosphorylation of the kinase protein.

Chapter 3: Results

3.1 *EMS1* genetically interacts with *SERK1*

3.1a Identification of the *EMS1* weak allele *ems1-2*

In order to obtain *EMS1* weak alleles with only partially reduced *EMS1* expression, multiple lines with T-DNA insertions within the promoter region of *EMS1* were ordered from the Signal Collection of the Salk institute. After examination of *EMS1* gene expression level alteration by RT-PCR, one line (SALK_051989) with T-DNA insertion 597 bp upstream of the *EMS1* start codon showed considerably reduced *EMS1* expression (Fig 3.1A). This new allele was named *ems1-2* afterwards and used as a weak allele in this study.

In initial phenotypic analyses, *ems1-2* plants did not show any obvious notable defects. However, it was noticed that *ems1-2* plants were sensitive to environmental conditions and showed slightly reduced fertility (Fig 3.1E) when grown in less favorable environments, such as weak light intensity and high temperature. After further more detailed examination, a small numbers of nonviable pollen grains could occasionally be seen in *ems1-2* anthers (Fig 3.1C). However, no specific environmental factors were identified as the certain cause of the variable phenotype of *ems1-2*.

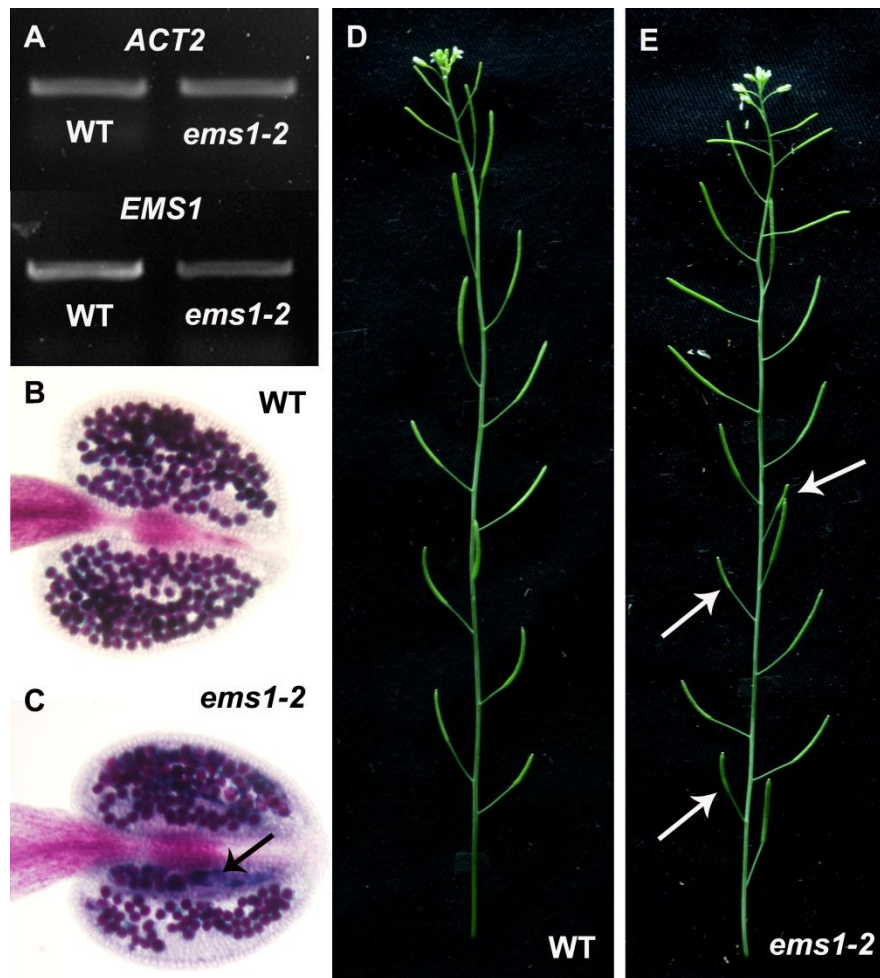


Fig3.1 *ems1-2* is a weak allele of *EMS1*.

(A) Expression level of *EMS1* and *ACT2* genes in wild type and *ems1-2* plants. *EMS1* gene expression is reduced in *ems1-2* young inflorescences, as indicated by RT-PCR. Upper panel: *ACT2*, 22 cycles; lower panel: *EMS1*, 28 cycles. *ACT2* gene serves as internal control.

(B) Pollen staining in wild-type anther, showing normally developed viable pollen grains which are stained into red color.

(C) Pollen staining of *ems1-2* anther. Nonviable pollen grains (arrows) can be occasionally produced, as indicated by the blue color after pollen staining. By contrast, healthy and viable pollen grains are stained bright red in color.

(D) The main branch of a wild- type plant, showing fully elongated siliques.

(E) The main branch of an *ems1-2* plant, showing sterile siliques (arrows) occasionally produced, which do not elongate due to fertilization failure.

3.1b *ems1-2 serk1-1* double mutants show significant fertility reduction

The newly identified *ems1-2* weak allele was used to generate *ems1-2 serk1-1* and *ems1-2 serk2-1* double mutants by crossing. The F₂ seeds were planted for observation of potential phenotypes. In F₂ populations from the above two crosses, only the *ems1-2 serk1-1*, but not the *ems1-2 serk2-1* plants showed significant fertility reduction, which was not seen in either single mutant. This result clearly indicated that the *SERK1* mutation enhanced the mild phenotype of *ems1-2*, via the genetic interaction between the *EMS1* and *SERK1* genes.

It was noticed that the first 15 siliques produced by *ems1-2 serk1-1* plants were mostly sterile (Fig3.2B, D). The failure of silique elongation suggested unsuccessful fertilization within the carpels. However, it was also noticed that fertility could be gradually recovered in the late life stages of *ems1-2 serk1-1* plants. In other words, although great fertility loss was observed, no completely sterile *ems1-2 serk1-1* plants

were found in the entire population. PCR genotyping was performed to determine the genetic backgrounds of those plants with partially sterile phenotypes, confirming that they were all *ems1-2 serk1-1* plants. Seeds collected from *ems1-2 serk1-1* plants gave rise to plants showing identical partially sterile phenotypes, indicating this phenotype is inheritable. Consistent results were obtained from more than 5 consecutive generations of *ems1-2 serk1-1*.

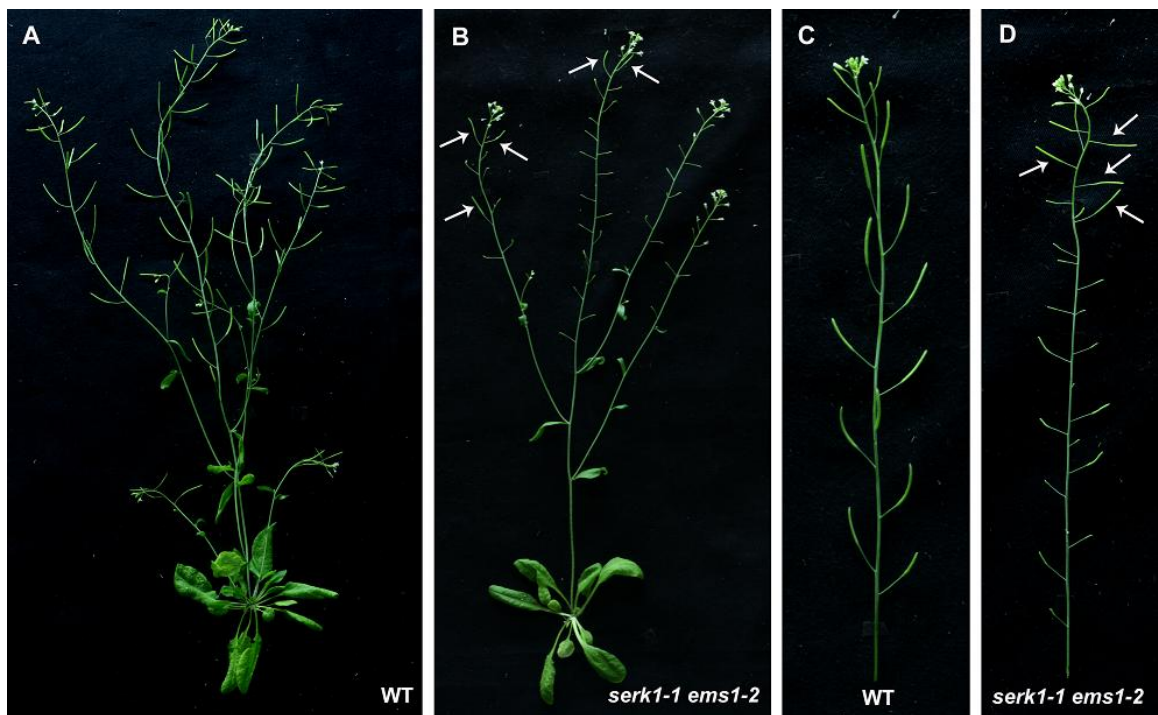


Fig3.2. *serk1-1 ems1-2* double mutants show significant fertility reduction

(A) Wild-type plant (Col-0) shows normal fertility, as indicated by fully developed siliques with normal elongation.

(B) *ems1-2 serk1-1* double mutant shows significantly reduced fertility, with only few fertile siliques (arrows), as indicated by their normal length after elongation.

(C) The main branch from a wild-type plant (Col-0), showing that all siliques are normally elongated and fertile.

(D) The main branch from an *ems1-2 serk1-1* double mutant, showing mostly sterile siliques without elongation. The fertile siliques are indicated by arrows.

In order to get a clearer understanding of the fertility loss in *ems1-2 serk1-1*, fertility was evaluated in this line. Individual siliques were counted on 30 individual *ems1-2 serk1-1* plants (Fig3.3A, B). The first 20 siliques produced on the main branch of each plant were examined for fertility. Siliques showing normal full elongation were recorded as fertile. Siliques showing partial elongation with reduced lengths were recorded as semi-sterile. Semi-sterile siliques were still able to set seeds, but in fewer numbers than wild-type plants. Siliques with a complete lack of elongation were recorded as sterile.

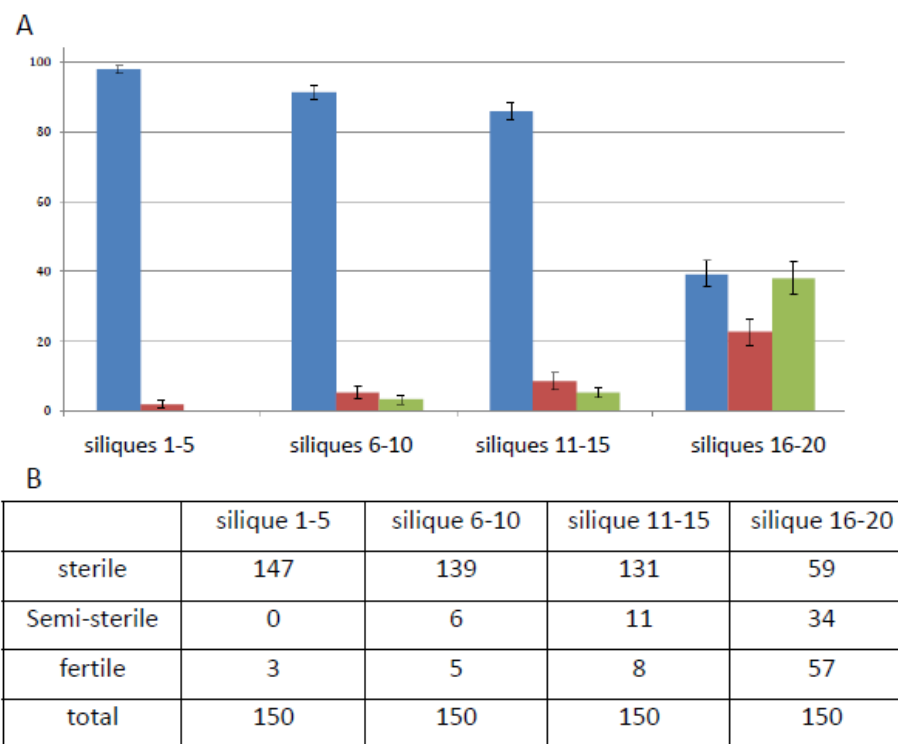


Fig 3.3 Fertility loss and recovery in *ems1-2 serk1-1* plants

(A) Fertility evaluation of the first 20 siliques produced in each of the 30 individual *ems1-2 serk1-1* plants, represented in percentage. Every five siliques were grouped as a subunit, beginning at the base of the main branch. Fertile siliques are indicated in green color, while sterile and semi-sterile siliques are shown in blue and brown color, respectively. Y axis numbers are shown in percentage. Standard error bars are shown.

(B) Original data collected from 30 individual *ems1-2 serk1-1* plants.

Early flowers produced by *ems1-2 serk1-1* plants showed differences in anther phenotype when observed by light microscopy, as compared to wild-type plants. Anthers appeared in grayish or even black color and were smaller in size (Fig3.4B) compared with those in the wild type plants (Fig3.4A). The anther epidermis looked flat and smooth, which was also not seen in wild-type anthers at equivalent developmental stages. No released pollen grains were seen outside the mutant anthers, and anther dehiscence was also not observed.

After further examination of pollen production in *ems1-2 serk1-1* by pollen staining, early flower buds from *ems1-2 serk1-1* double mutants showed severe defects in pollen production. Pollen production failure was observed and represented by phenotypes of multiple kinds. In anthers showing the strongest mutant phenotype, seen in the earliest produced buds, no pollen grains were produced in any the four lobes in each anther (Fig3.4E). For weaker phenotypes, fewer numbers of viable pollen grains, compared with wild type plants, were produced in some anther lobes, while nonviable pollen grains were also seen in the same anther (Fig3.4D, F). The phenotype went from strong to weak and finally became undistinguishable from wild-type plants based on an indeterminate manner of the production of flower buds, which was correlated to the partial fertility loss phenotype. By contrast, no significant pollen production defects were observed in Col-0 wild type, *ems1-2* and *serk1-1* plants.

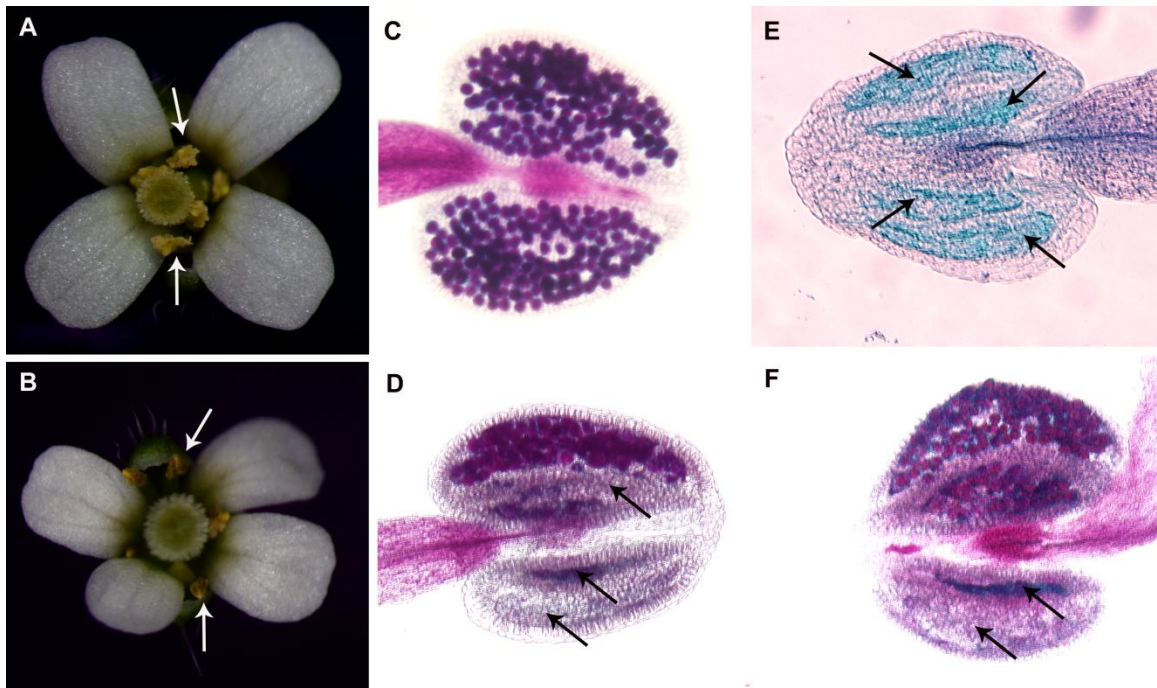


Fig3.4. *ems1-2 serk1-1* double mutant flowers show defects in pollen production

(A) Flower of a wild-type plant (Col-0). Anthers produce and release pollen grains after dehiscence (arrows). Pollen grains yellow in color can be seen on the stigma as well as on anther epidermis.

(B) Flower of *ems1-2 serk1-1* double mutant. Anthers fail to produce pollen grains and show abnormal black color (arrows). Epidermis of the anthers show a smooth and flat appearance, with no dehiscence observed.

(C) Wild type anther after pollen staining, showing viable pollen grains stained bright red in color.

(D) (E) (F), *ems1-2 serk1-1* double mutant anthers after pollen staining, showing partial or complete empty lobes without viable pollen grains. Unhealthy and nonviable pollen grains are stained blue in color.

3.1c *ems1-2 serk1-1* plants showed defects in anther cell development

After checking semi-thin sections of stage 5 anthers from *ems1-2 serk1-1* (Fig3.5D), defects in anther cell development were observed. Slightly increased numbers of microsporocytes were noticed when compared to wild-type plants (Fig3.5A), which was similar to the phenotype of *ems1* anthers (Fig3.5B). Additionally, no complete tapetum layer could be identified. Some cells showed abnormal morphological characteristics different from typical tapetal cells. It appeared that some cells in the position of microsporocytes or tapetum failed to fully establish their identity as a specific cell type. Both *ems1-2* and *serk1-1* showed normal anther cell development, with five fully differentiated cell types in each anther lobe.

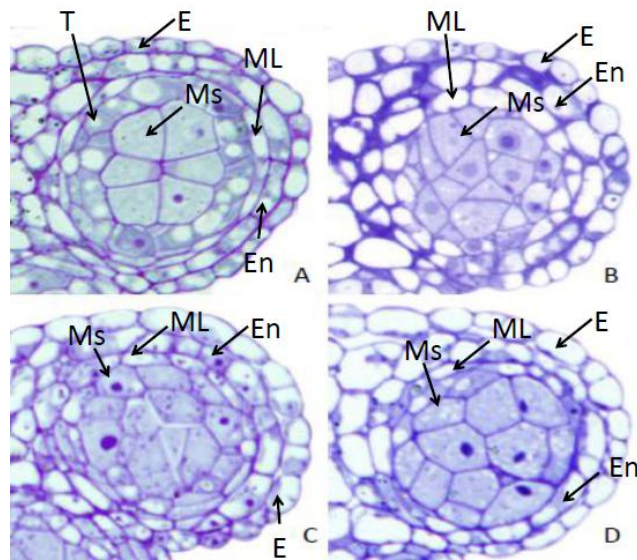


Fig3.5. *ems1-2 serk1-1* double mutants are defective in anther cell development

(A). Semi-thin section picture of a Col-0 wild-type anther lobe at stage 5 of development, showing 5 well differentiated cell types. Central microsporocytes (Ms) are surrounded by four somatic cell layers: tapetum (T), middle layer (ML), endothecium (En) and epidermis (E).

(B). Semi-thin section picture of an *ems1-1* anther lobe at stage 5, showing extra numbers of microsporocytes and no tapetum.

(C). Semi-thin section picture of a *serk1-1serk2-1* anther lobe at stage 5, showing extra numbers of microsporocytes and no tapetum.

(D). Semi-thin section pictures of a *serk1-1 ems1-2* anther lobe at stage 5, showing abnormally developed microsporocytes and tapetum. No continuous tapetum layer can be

recognized. Morphological features different from typical tapetal cells can be seen from cells in the position of tapetum.

3.1d *ems1 serk1-1 serk2-1* showed phenotype identical to *ems1* and *serk1-1 serk2-1*

Samples from triple mutant *ems1 serk1-1 serk2-1* were prepared for anther semi-thin section analysis. After comparing with *ems1* (Fig3.6B) and *serk1-1 serk2-1* (Fig3.6C), semi-thin sections of stage 5 anthers from *ems1 serk1-1 serk2-1* (Fig3.6D) showed very similar phenotype as these two mutants. All three kinds of mutants showed extra numbers of microsporocytes and a missing tapetum. The copied phenotype in *ems1 serk1-1 serk2-1* further supported our main hypothesis that *EMS1* and *SERK1/2* work in the same signaling pathway.

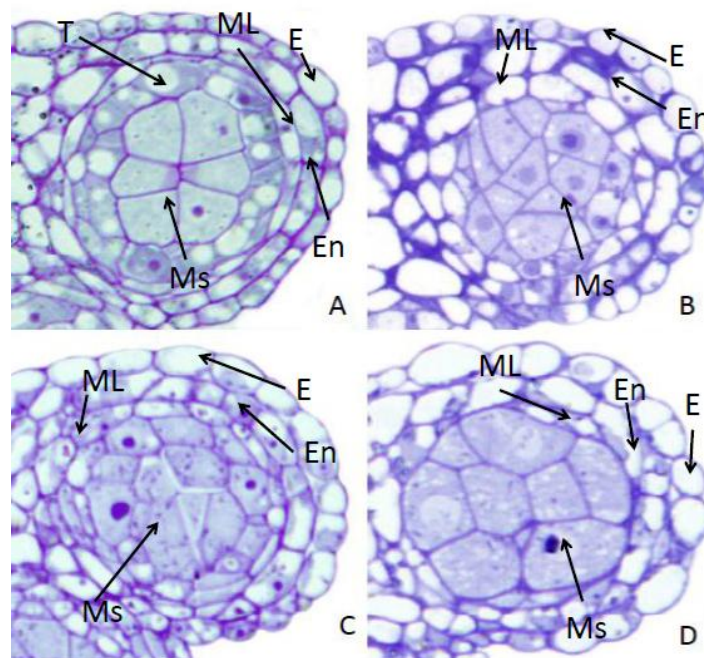


Fig3.6. *ems1 serk1-1 serk2-1* triple mutants show identical phenotype as *ems1* and *serk1-1 serk2-1*.

(A) Semi-thin section picture of a Col-0 wild type anther lobe at stage 5 of development, showing 5 well differentiated cell types. Central microsporocytes (Ms) are surrounded by four somatic cell layers: tapetum (T), middle layer (ML), endothecium (En) and epidermis (E).

(B) Semi-thin section picture of an *ems1* anther lobe at stage 5, showing extra microsporocytes and no tapetum.

(C) Semi-thin section picture of a *serk1-1 serk2-1* anther lobe at stage 5, showing extra microsporocytes and no tapetum.

(D) Semi-thin section picture of a *ems1 serk1-1 serk2-1* anther lobe at stage 5, showing extra microsporocytes and no tapetum.

3.1e EMS1 signaling is dependent on SERK1/2 function

Our previous studies discovered that *AtMLI::TPD1* overexpression can promote anther cell proliferation in wild type plants, resulting in the production of extra cell layers in the position of the tapetum and middle layer (Huang, unpublished data). It was also

observed that this phenotype requires the normal function of *EMS1*, since no extra cell proliferation occurred in *AtML1::TPD1 / ems1* plants.

In order to test whether the *AtML1::TPD1* overexpression phenotype is also *SERK1/2* dependent, *AtML1::TPD1 / serk1-1 serk2-1* plants were generated for examination of anther semi-thin sections.

After examining the stage 5 anther semi-thin sections from *AtML1::TPD1 / serk1-1 serk2-1* plants (Fig3.7C), instead of showing extra cell layers due to abnormal cell proliferation (Fig3.7B), a phenotype identical to that of the *serk1-1 serk2-1* double mutant was observed. The *AtML1::TPD1 / serk1-1 serk2-1* anther phenotype provides strong genetic evidence that *EMS1/TPD1* signaling requires normal *SERK1/2* function in the anther. It also suggests that all of these four genes are integrated within the same signaling pathway.

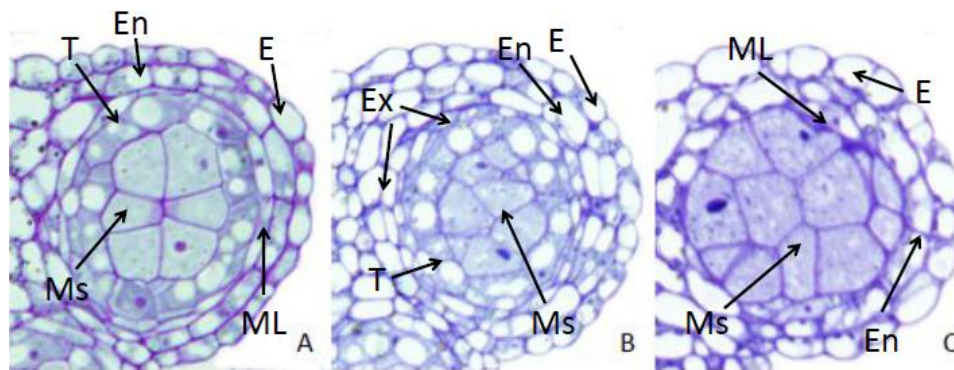


Fig3.7. *AtML1::TPD1* overexpression triggers abnormal anther cell proliferation in Col-0 wild type, but not in *serk1-1 serk2-1* double mutants

(A) Semi-thin section picture of a Col-0 wild type anther lobe at developmental stage 5, showing 5 well differentiated cell types. Central microsporocytes (Ms) are surrounded by four somatic cell layers: tapetum (T), middle layer (ML), endothecium (En) and epidermis (E).

(B) Semi-thin section picture of a *AtML1::TPD1*/Col-0 anther lobe at stage 5, showing extra cell layers (Ex) in the positions of tapetum (T) and middle layer (ML) due to abnormal anther cell proliferation.

(C) Semi-thin section picture of a *AtML1::TPD1/serk1-1 serk2-1* anther lobe in stage 5, showing phenotype identical to *serk1-1 serk2-1*, as previously shown in Fig 3.5c and Fig 3.6c

3.1f *SERK1* and *SERK2* play partially redundant yet unequally important roles during anther development in *Arabidopsis*

Our previous phenotypic analysis of *ems1-2 serk1-1* and *ems1-2 serk2-1* provided genetic evidence which supports the idea that *SERK1* and *SERK2* play redundant roles of unequal importance during *Arabidopsis* anther development. We then performed a promoter swap complementation test to examine the cause of unequal contributions of *SERK1* and 2 during anther development. We also demonstrated that

ectopic overexpression of *SERK2* was sufficient to rescue the fertility loss in *ems1-2 serk1-1*.

The ectopic expression of *SERK1::SERK2* or *SERK2::SERK1* was able to partially restore fertility in *serk1-1 serk2-1* plants, ranging from nearly complete restoration of fertility to partial complementation (Table3.1). A few transformants still exhibited sterility. Based on the fertility data from 30 transformants of both kinds, it was noticed that the ectopic expression of *SERK2::SERK1* yielded better complementation compared with *SERK1::SERK2*, which yielded more partially complemented transformants and fewer transformants that were almost completely fertile.

Table 3.1 Complementation effect of *SERK1::SERK2* and *SERK2::SERK1* in *serk1-1 serk2-1* background

Expression Type	Fertile Plants	Semi-sterile Plants	Sterile Plants
<i>SERK1::SERK2</i>	9	14	7
<i>SERK2::SERK1</i>	18	9	3

The expression of either *SERK1::SERK2* or *SERK2::SERK2* was able to mostly restore or partially rescue the severe fertility loss in *ems1-2 serk1-1* plants (Table3.2). It also suggested that overexpression of either *SERK1* or *SERK2* is sufficient to maintain anther development regulation, provided that *EMS1* expression is not completely

abolished. Possible difference between *SERK1* and *SERK2* expression domains may not be the most critical factor here, which gives rise to the similar but different physiological functions of *SERK1* and *SERK2*.

Table 3.2 Complementation effect of *SERK1::SERK2* and *SERK2::SERK2* in *ems1-2 serk1-1* background

Expression Type	Fertile Plants	Mostly Fertile Plants	Mostly Sterile Plants
<i>SERK1::SERK2</i>	14	11	5
<i>SERK2::SERK2</i>	12	15	3

3.2 SERK1 biochemically interacts with EMS1 in *Arabidopsis*

3.2a SERK1 specifically interacts with EMS1 in *Arabidopsis* protoplasts

After co-transfection of *Arabidopsis* protoplasts using EMS1 and SERK1, each fused with half EYFP, signals from complemented EYFP were observed during confocal microscopy examination (Fig3.8 D, E, F). Meanwhile, no signals were detected between the control protein pair (EMS1 and BAK1, Fig3.8 A, B, C), which indicated that the interaction between the EMS1 and SERK1 pair is specific.

We fused half EYFPs to both the N-terminal and C-terminal regions of EMS1 and SERK1 and tested N-terminal fusion pair and C-terminal fusion pair separately. EYFP signals were detected in both versions when examined using our BiFC system.

However, it was noticed that the C-terminal fusion pair yielded relatively stronger EYFP signal compared with N-terminal fusion pair.

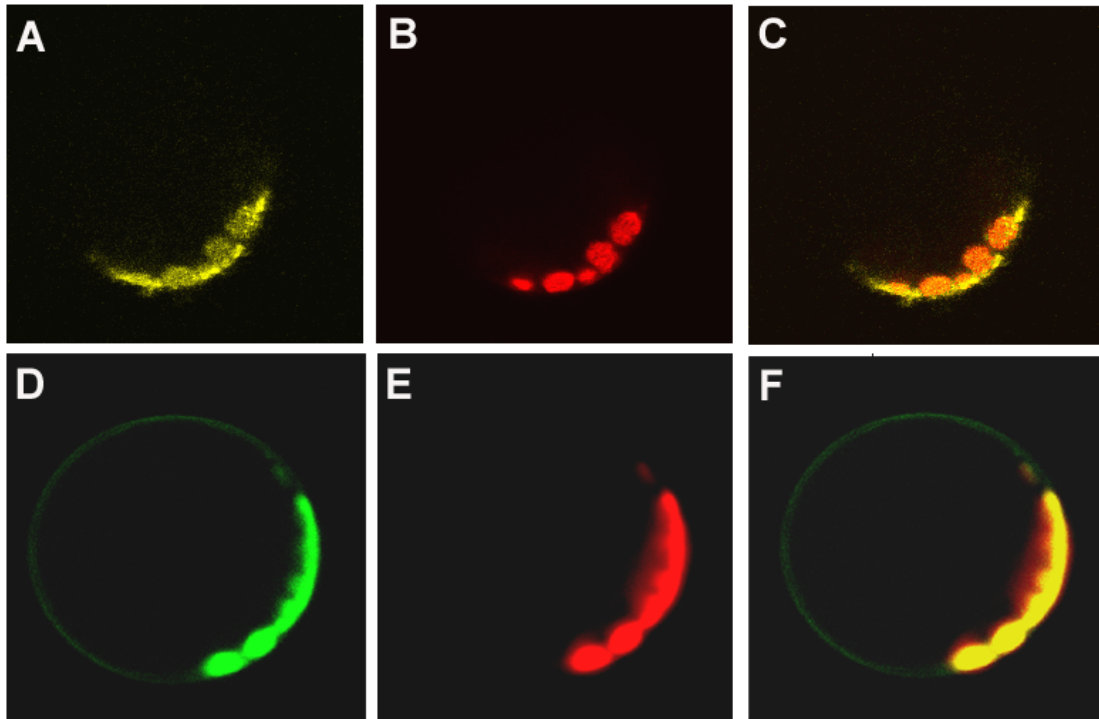


Fig 3.8 SERK1 specifically interact with EMS1 in *Arabidopsis* protoplasts

(A) (B) (C) EMS1-cEYFP + BAK1 (SERK3)-nEYFP

(D) (E) (F) EMS1-cEYFP + SERK1-nEYFP

(A) (D) YFP channel

(B) (E) Autofluorescence

(C) (F) Overlay, showing no signal on the membrane (C) and the signal (F) from complemented EYFP on the membrane as a result of EMS1-SERK1 interaction.

3.2b Interaction between truncated EMS1 and SERK1 in *Arabidopsis* protoplasts

In order to dissect the functional domains responsible for the interaction between EMS1 and SERK1, truncated EMS1 and SERK1 versions without kinase domains were each fused with half EYFP in C-terminal regions. The resulting proteins, EMS1-LRR-TM-cEYFP and SERK1-LRR-TM-nEYFP, were co-expressed in *Arabidopsis* protoplasts. For the negative control, TPD1-cEYFP and SERK1-LRR-TM-nEYFP pair was used (Fig3.9 A, B, C).

Signal from complemented EYFP was observed during confocal microscopy examination between EMS1-LRR-TM-cEYFP and SERK1-LRR-TM-nEYFP (Fig3.9 D, E, F). This result indicated that kinase domains are not required for the EMS1-SERK1 interaction in *Arabidopsis* protoplasts.

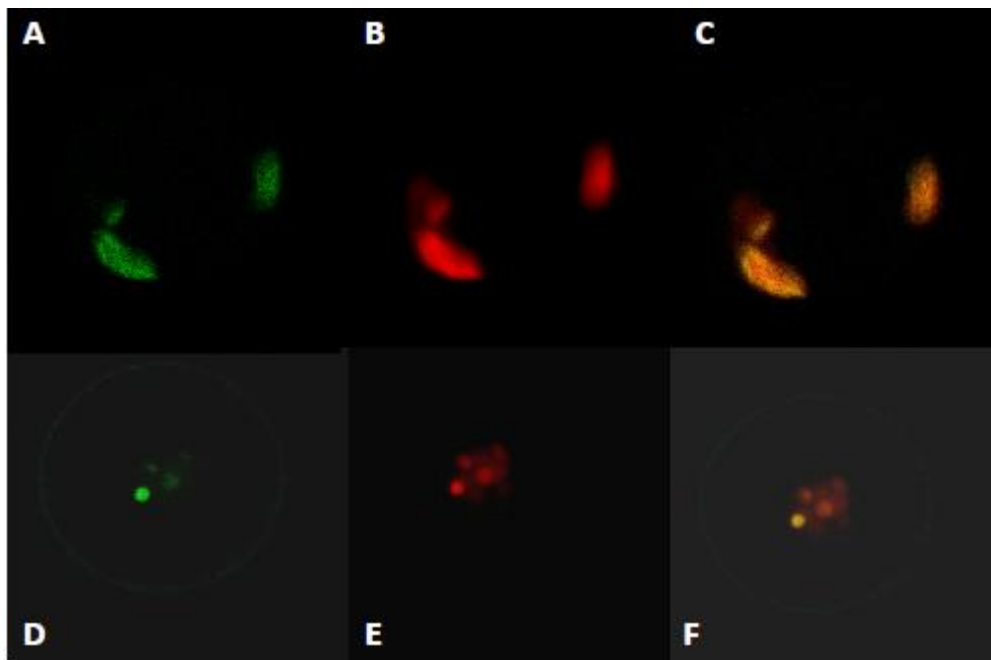


Fig 3.9 Kinase domains are not essential for interaction between SERK1 and EMS1 in *Arabidopsis* protoplasts.

(A) (B) (C) TPD1-cEYFP + SERK1-LRR-TD -nEYFP.

(D) (E) (F) EMS1-LRR-TM-cEYFP + SERK1-LRR-TM-nEYFP.

(A) (D) YFP channel

(B) (E) Autofluorescence

(C) (F) Overlay, showing no signal on the membrane (no interaction) or signal from complemented EYFP on the membrane as a result of LRR domains interaction between EMS1 and SERK1.

3.2c The ligand protein TPD1 is not required for SERK1-EMS1 interaction in *Arabidopsis* protoplasts

In order to examine the role of TPD1, ligand of EMS1, during the interaction between EMS1 and SERK1, we prepared *Arabidopsis* protoplasts using leaves from *tpd1* mutants, in which no TPD1 proteins are produced. We were also able to observe the signal from complemented EYFP only from the EMS1-cEYFP/SERK1-nEYFP pair (Fig3.10 D, E, F), but not from EMS1-cEYFP + BAK1-nEYFP pairs (Fig3.10 A, B, C). This result indicated that EMS1 and SERK1 can specifically interact with each other in *Arabidopsis* protoplasts without the presence of TPD1 ligand protein.

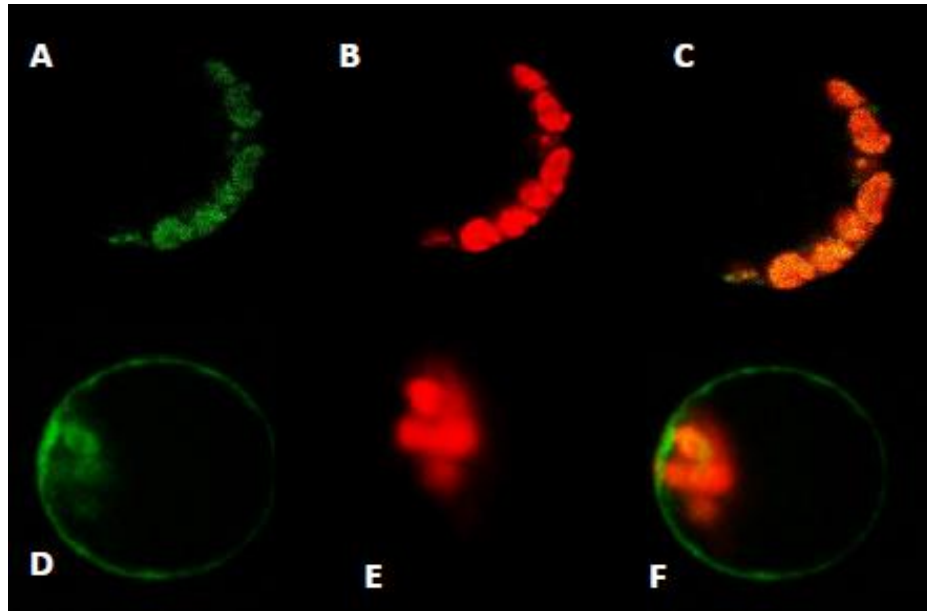


Fig 3.10 SERK1 interacts with EMS1 in *Arabidopsis* protoplasts prepared from *tpd1* plants.

(A) (B) (C) EMS1-cEYFP + BAK1(SERK3)-nEYFP in protoplasts prepared from *tpd1* plants.

(D) (E) (F) EMS1-cEYFP + SERK1-nEYFP in protoplasts prepared from *tpd1* plants.

(A) (D) YFP channel

(B) (E) Autofluorescence

(C) (F) Overlay, showing no signal on the membrane (C) and the signal (F) from complemented EYFP on the membrane as a result of EMS1-SERK1 interaction.

3.2d Homodimerization observed between SERK1 but not EMS1 proteins in *Arabidopsis* protoplasts

Although in the working model we proposed, EMS1 works as a heterodimer with either SERK1 or SERK2, we also examined the possibility of EMS1 or SERK1 homodimerization in *Arabidopsis* protoplasts.

Each half of the EYFPs was fused to the C-terminal regions of EMS1 or SERK1 protein pairs. Complemented EYFP signals were observed only between SERK1 (Fig3.11 D, E, F) but not EMS1 pairs (Fig3.11 A, B, C).

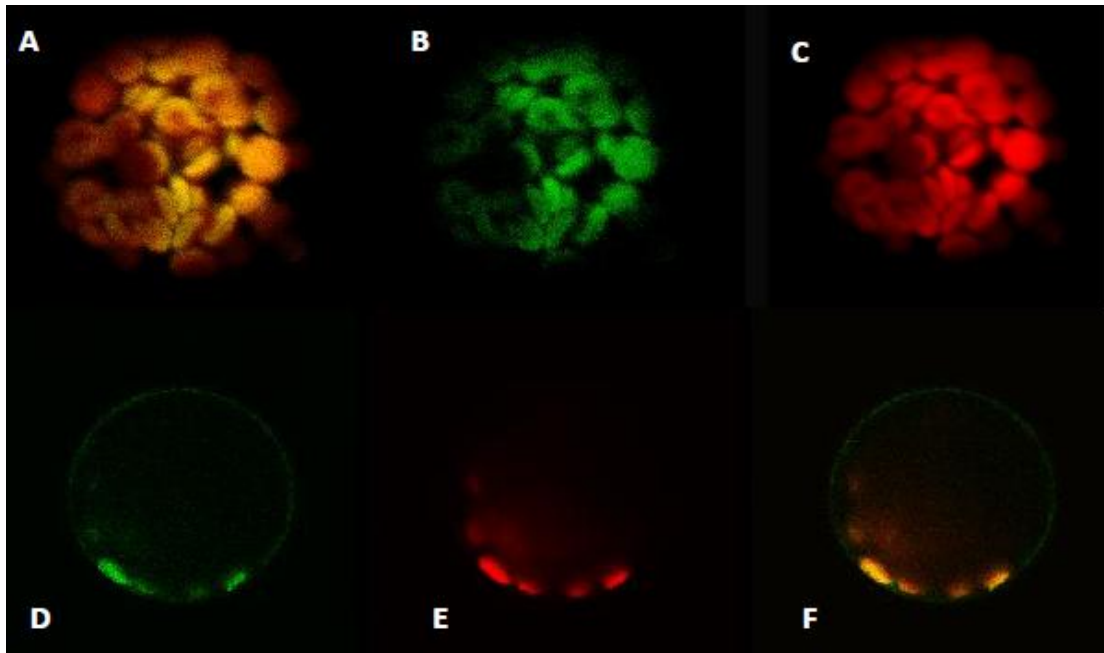


Fig 3.11 SERK1 but not EMS1 proteins form homodimers in *Arabidopsis* protoplasts

(A) (B) (C) EMS1-cEYFP + EMS1-nEYFP in protoplasts

(D) (E) (F) SERK1-cEYFP + SERK1-nEYFP in protoplasts

(A) (D) YFP channel

(B) (E) Autofluorescence

(C) (F) Overlay, showing no signal on the membrane (C) and the signal (F) from complemented EYFP on the membrane as a result of SERK1 homodimerization.

3.3 Functional analysis of EMS1 phosphorylation

3.3a Transphosphorylation occurs between kinase domains of EMS1 and SERK1

After confirming the interaction between EMS1 and SERK1 using the BiFC system, we then further looked into the role of phosphorylation during the interaction.

GST-EMS1-KD and His-SERK1-KD recombinant proteins were purified and used for in vitro autophosphorylation and transphosphorylation of EMS1 and SERK1. In order to evaluate the phosphorylation levels of the proteins, γ -³³P labeled ATP was used during the kinase assay.

As indicated by the radioautography gel result, GST-EMS1-KD (Fig3.12C) and His-SERK1-KD (Fig3.12B) are able to phosphorylate each other during in vitro kinase assay, thus increasing the phosphorylation levels of both proteins when compared with their autophosphorylation levels (Fig3.12A).

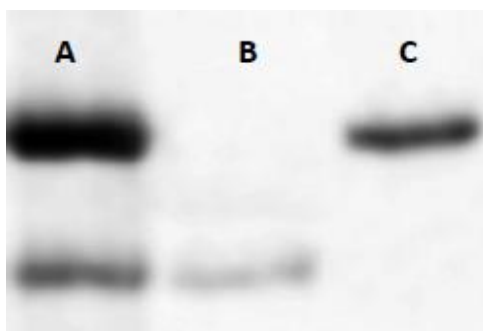


Fig 3.12 *In vitro* autophosphorylation and transphosphorylation of GST-EMS1-KD and His-SERK1-KD proteins (radioautography gel scanning)

Equal amount of protein sample was loaded in each lane.

Lane A: transphosphorylation between of GST-EMS1-KD and His-SERK1-KD

Lane B: autophosphorylation of His-SERK1-KD

Lane C: autophosphorylation of GST-EMS1-KD

3.3b K945E mutation does not abolish *in vitro* autophosphorylation activity in GST-EMS1-KD.

Based on the computational and experimental evidence, we introduced the K945E mutation into GST-EMS1-KD, trying to abolish autophosphorylation of the protein for transphosphorylation study purposes. GST-EMS1-KD (K945E) and native GST-EMS1-KD proteins were purified before being subjected to the *in vitro*

phosphorylation assay to evaluate the possible autophosphorylation difference between the two.

However, we were surprised to find that, the K945E mutation did not completely abolish autophosphorylation of GST-EMS1-KD. Based on the radioautography gel scanning, the K945E mutation only caused a moderate decrease of autophosphorylation activity (Fig3.13A, B).

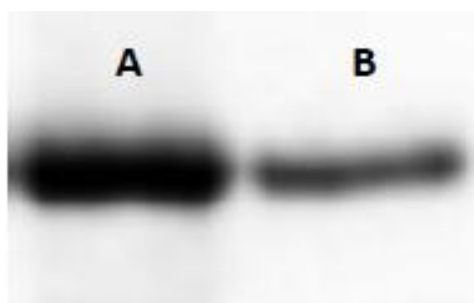


Fig 3.13 *In vitro* autophosphorylation activity is not disrupted after introducing K945E mutation into GST-EMS1-KD (radioautography gel scanning)

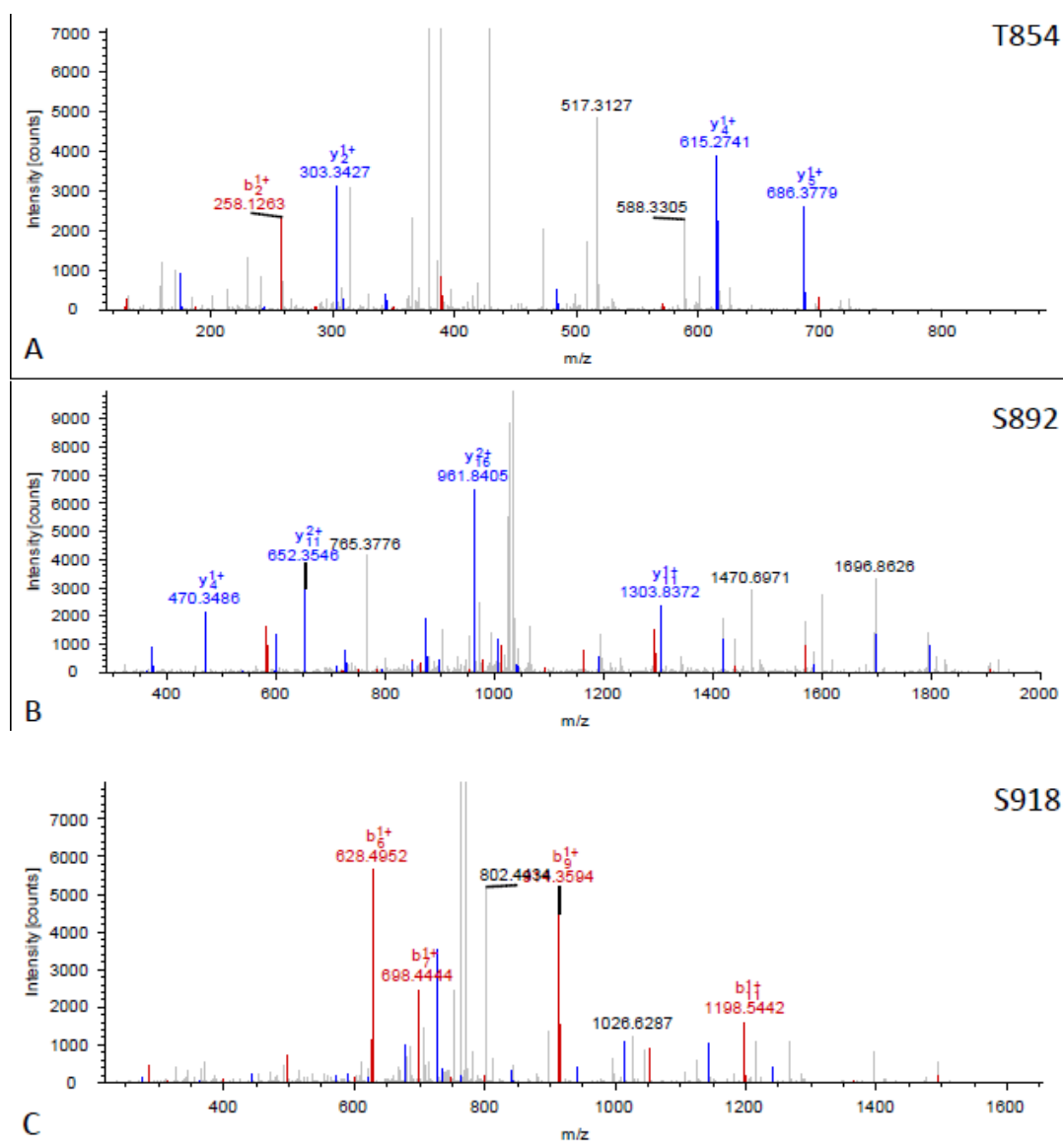
Equal amount of protein sample was loaded in each lane.

Lane A: autophosphorylation of GST-EMS1-KD (wild type)

Lane B: autophosphorylation of GST-EMS1-KD (K945E)

3.3c Identification of *in vitro* phosphorylation sites within GST-EMS1-KD

Fig 3.14 GST-EMS1-KD recombinant protein is phosphorylated on multiple serine/threonine residues *in vitro*.



D

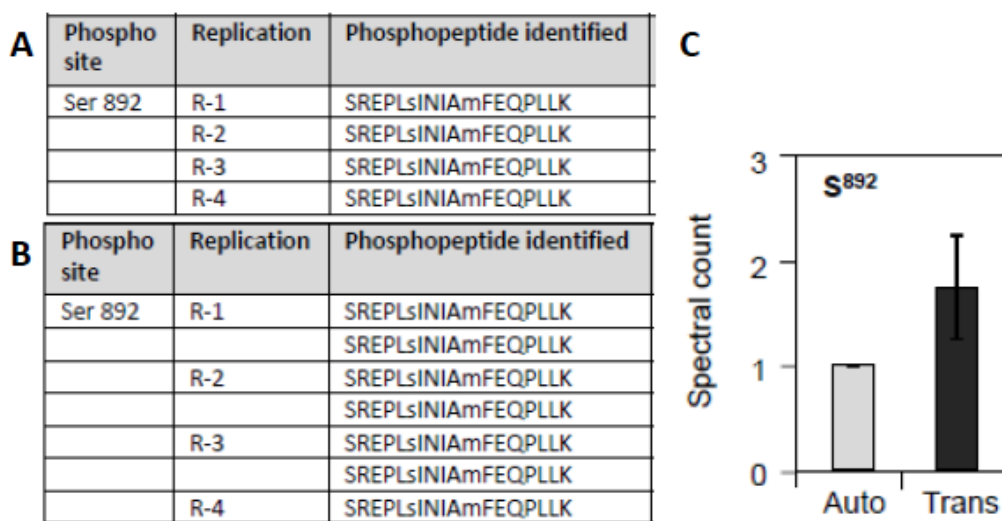
851	WAMTKRVKQR	DDPERMEESR	LKGFVDQNLV	FLSGRSREP	LSINIAMFEQ
901	PLLKVRLGDI	VEATDHFSSK	NIIGDGGFGT	VYKACLPGEK	TVAVKKLSEA
951	KTQGNREFMA	EMETLGKVKH	PNLVSLGVC	SFSEKLVVY	EYMVNGSLDH
1001	WLRNQTGMLE	VLDWSKRLKI	AVGAARGLAF	LHGFIPHII	HRDIKASNIL
1051	LDGDFEPKVA	DFGLARLISA	CESHVSTVIA	GTFGYIPPEY	GQSARATTKG
1101	DVYSGVILL	ELVTGKEPTG	PDFKESEGGN	LVGWAIQKIN	QGKAVDVIDP
1151	LLVSVALKNS	QLRLLQIAML	CLAETPAKRP	NMLDVLKALK	EI

(A)(B)(C) LC/MS/MS identification of three phosphorylation *in vitro* sites, T854, S892 and S918, within GST-EMS1-KD.

(D) Identified serine/threonine residues are indicated in red color. Residues detected within the activation loop region are also underlined.

Multiple phosphorylated serine/threonine residues were identified by LC/MS/MS analysis of the GST-EMS1-KD *in vitro* phosphorylation assay sample (Fig3.14D). In the juxtamembrane region, 8 phosphorylated residues were detected: T854, S869, S883, S892, T914, S918, T930 and T941 (Fig3.14 A, B, C). Two phosphorylated residues were identified within the activation loop region: S1076 and T1077. S1160 was the only residue detected with phosphorylation modification near to the carboxyl terminal.

Fig 3.15 Quantitative enhancement of phosphorylation in GST-EMS1-KD protein after His-SERK1-KD transphosphorylation *in vitro*



(A) Detection of phosphopeptide including residue S892 from GST-EMS1-KD *in vitro* autotransphosphorylation sample.

(B) Detection of phosphopeptide including residue S892 from GST-EMS1-KD *in vitro* transtransphosphorylation sample.

(C) Enhanced phosphorylation on residue S892 in GST-EMS1-KD after His-SERK1-KD transphosphorylation *in vitro*.

After LC/MS/MS analysis, quantitative enhancement of phosphorylation was observed in GST-EMS1-KD *in vitro* trans-phosphorylation samples (Fig3.15A, B, C). It was reflected by increased detection frequency of phosphopeptides, most typically on residue S892. This discovery also provided support to the radioautography result of His-SERK1-Kd and GST-EMS1-KD *in vitro* transphosphorylation. Similar effect has been reported previously for BRI1-BAK1 transphosphorylation (Wang et al., 2008).

Chapter 4: Discussion

4.1 Functional redundancy between SERK1 and SERK2

It has been proposed that LRR-RLKs from the SERK protein family share functional redundancy due to the high similarity of their amino acid sequences. In the working model proposed in this study, SERK1 and SERK2 both work as co-receptors of EMS1 in a protein complex, playing redundant and interchangeable roles.

It has been demonstrated that the kinase domains from SERK family proteins show different levels of autophosphorylation intensities during *in vitro* kinase assays. SERK1 shows a higher autophosphorylation activity than SERK2 (Karlova et al., 2010).

In our genetic studies, we have also observed that, in the promoter swap complementation experiment, *SERK1* yielded better complementation effect compared with *SERK2*, driven by either its native promoter or the *SERK2* promoter. Meanwhile, *SERK2* ectopic expressions driven by either its native promoter or the *SERK1* promoter yielded similar fertility rescue effect in *ems1-2 serk1-1*. It is certain that *SERK1/2* share functional redundancy in *EMS1* signaling pathway since overexpression of *SERK2* restored fertility in *ems1-2 serk1-1*. It has also been reported that either *SERK1* or *SERK2* expression is able to rescue the sterility in *serk1-1 serk2-1* mutants (Albrecht et al., 2005; Colcombet et al., 2005).

Taken together, it is very likely that SERK1 is functionally more important than SERK2 due to its biochemical nature rather than their expression domain differences. Being more heavily phosphorylated, SERK1 may be more efficient in the signal relay to downstream molecules, and thus can be more significant for the signal output in the *EMS1* signaling pathway.

However, there is an interesting question to ask about the function of SERK1 and SERK2. As candidate co-receptors of multiple LRR-RLKs with diverse functions, what is the mechanism for SERK proteins to specify the exact way that they should work when they play dual or even multiple roles? SERK1 and BAK1 are two ready examples from the SERK family, which both serve as co-receptors of BRI1. It would be a reasonable guess that they as adapters that connect different signaling pathways by specifying the signals they receive and responding accordingly.

4.2 Role of TPD1 during EMS1-SERK1/2 interaction

As the ligand of EMS1, TPD1 is proposed to play a particular role during the interaction between EMS1 and SERK1/2. However, in our BiFC assays using the *Arabidopsis* protoplast system, EMS1 and SERK1 could specifically interact with each other both with and without the presence of TPD1. It is also noted that in a previous study using the luciferase complementation imaging (LCI) method, which works in a similar manner as BiFC, the *Arabidopsis* receptor-like kinase CORYNE (CRN) could form

homodimers as well as heterodimers with LRR-RLK CLV2 in the absence of CLV3 peptide, the proposed ligand of CLV2 (Bleckmann et al, 2010; Zhu et al 2010).

It has been noted that both LCI and BiFC will lead to transient protein expression at levels which may be much higher than native expression in plants. If the function of a ligand during complex formation is to stabilize the protein complex or facilitate its formation, it is very unlikely to be reflected in a mimic system like LCI or BiFC, in which protein complexes can be formed much easier due to the abundance of proteins in the protoplasts. Another possible explanation is that the EMS1 protein complex is assembled independent of TPD1 binding, but may require its activation in order to introduce conformational change before performing its full function.

The significance of TPD1 binding to the LRR domain of EMS1 is another interesting question to explore. It is not yet clear whether the initiation of the EMS1 protein complex occurs before or after TPD1 binding, which may either trigger the recruitment of SERK1/2 or activate the preassembled EMS1 protein complex.

In BR signaling, the BR receptor BRI1 only becomes active after the binding of BR, which triggers the recruitment of its co-receptor BAK1 and phosphorylation on its inhibitor protein BKI1, which then disassociate with BRI1 (Wang et al.,2006). Unlike BRI1, EMS1 does not have a typical C-terminal tail. However, it is possible that the domain near the C-terminal region of EMS1 also works as a protein interacting domain, although not very likely with an inhibitor protein similar to BKI1, since a site mutation in

this region has been reported to completely abolish EMS1 function in the *exs-1* allele (Canales et al., 2002).

4.3 Working model of the EMS1-SERK1/2 protein complex

As indicated by our BiFC result, unlike BRI1, EMS1 proteins are not able to form homodimers, which indicate it is more likely that one EMS1-SERK1/2 protein complex may work in the form of heterodimer, including one EMS1 protein molecule and one SERK1 or SERK2 protein molecule, which is functionally redundant with the other and interchangeable in the protein complex.

However, it is also possible that a tetramer could be formed via two different mechanisms. In the first case, the formation of the protein complex is initiated by the cross phosphorylation between EMS1 and SERK1/2. Increased level of EMS1 phosphorylation after EMS1-SERK1/2 interaction may change the conformation of EMS1 itself and facilitate the formation of EMS1 homodimers. This possibility cannot be ruled out since the BiFC system is not able to provide a mimic condition under which EMS1 proteins are more heavily phosphorylated. The second possible case is that SERK1/2, but not EMS1, may work as the molecular “glue” if any tetramers can be formed. Both our BiFC result and previous studies have already demonstrated that SERK1 dimers can be found in *Arabidopsis*. SERK1 may also capable of forming heterodimers with SERK2. The association between SERK1/2 homodimers / heterodimers may also be enhanced by increased phosphorylation levels of SERK1/2.

Ligand recognition and capture is another poorly understood mechanism in the EMS1 protein complex. In the better studied BRI1-BAK1/SERK1 protein complex, based on the crystal structure of LRR domains from BRI1 and SERK1, BRI1 is capable of forming the homodimers independent of BR binding (Santiago et al., 2013). As previously discussed here, this may also be the situation in the EMS1 protein complex. As the ligand of EMS1, TPD1 is a small protein and different in many ways from the simple compound BR, which is the ligand of BRI1. An island-like structure in the BRI1 LRR domain has been identified as the BR binding region. The EMS1 LRR domain does not include similar a structure and may form a different conformational structure for ligand binding. A previous study has found several EMS1 LRRs as the possible TPD1 interacting region (Jia et al., 2008). Computational studies can be helpful with more precise predictions and should be combined with biophysical methods in future studies.

4.4 Phosphorylation within the EMS1 kinase domain

The most unexpected discovery during our functional study of EMS1 phosphorylation is the effect of the mutation of K945E in EMS1, which failed to completely abolish autophosphorylation activity of the GST-EMS1-KD protein. As described previously, K945E is highly conserved among *Arabidopsis* LRR-RLKs and supposed to be critical for the conformational structure required for autophosphorylation activity. This is an indication that EMS1 phosphorylation may work in a less typical manner.

It is generally recognized that phosphorylation modification on kinase protein residues during protein interactions may have its function in two manners. Some are responsible for maintaining the autophosphorylation function of the kinase protein itself, which are typically two or three residues found within the activation loop of the kinase domain. Other residues in the juxtamembrane or C-terminal regions can facilitate interactions with other proteins by introducing conformation changes after phosphorylation modification.

Based on previous phylogenetic analyses, kinase domains from *Arabidopsis* LRR-RLKs have unique juxtamembrane domains as well as highly conserved activation loops, which are critical in maintaining autophosphorylation ability. Few serine or threonine residues are believed to be necessary in controlling autophosphorylation of the proteins. Only since very recently, *Arabidopsis* LRR-RLKs have been found capable of functioning as dual kinases with phosphorylation on both serine/threonine residues and tyrosine residues (Oh et al., 2009, 2010).

Among *Arabidopsis* LRR-RLKs, BRI1 and BAK1 are the only two examples so far that have their *in vivo* phosphorylation activities analyzed in depth. Researchers have also revealed phosphorylation on tyrosine residues in BRI1 and BAK and studied its physiological functions. Tyrosine phosphorylation in BRI1 is critical in controlling flowering time as well as releasing its inhibitor protein BKI1 from the membrane after disassociation.

Although we failed to detect any phosphorylation on tyrosine residues during our *in vitro* mapping effort in search of phosphorylation sites using GST-EMS1-KD, it is still possible for EMS1 tyrosine phosphorylation to function in *Arabidopsis*. Tyrosine phosphorylation may not occur *in vitro*, or may not be strong enough for detection from *in vitro* samples. Early works of BRI1 *in vitro* phosphorylation sites identification also failed to reveal the existence of tyrosine phosphorylation (Oh et al., 2000). It is possible to first examine the likely existence of tyrosine phosphorylation in planta using immunoblotting method.

The biggest problem in obtaining sufficient EMS1 protein samples from *in vivo* preparation is the lack of a stable system to produce EMS1 protein using plant materials in batch. It is mainly because of the specific function and expression pattern of the EMS1 protein, which is only found to be expressed and function in *Arabidopsis* anthers. Unlike EMS1, BRI1 works as a plant hormone receptor and is expressed widely in various plant tissues. Fused with epitope tags, BRI1 protein can be easily expressed and purified using liquid cultured suspension cells. This may be solved in the future through more efficient sample collection using more advanced separation methods or more sensitive detection techniques.

4.5 Potential molecules downstream of EMS1 signaling

The phenotype observed in old *ems1-2 serk1-1* anthers (Wang, unpublished result) has provided insight for the prediction of possible downstream molecules of EMS1 signaling. The recovery of fertility loss in the late life stage of *ems1-2 serk1-1* may be the

feedback regulation from some genes working downstream of *EMS1* in the signaling pathway, in response to greatly reduced *EMS1* signaling.

Additionally, we also observed abnormal anther cell development which was obviously not synchronized. This suggests that some genes involved in cell division cycle regulation are directly affected by impaired *EMS1* signaling. These may include some CDK genes, and/or genes encoding proteins critical for cell division such as cytoskeleton components

Based on semi-thin sections, some anther lobes showed degenerated cells in the center, while others showed delayed development of tapetum and microsporocytes. Developed pollen grains were also occasionally seen in some lobes, together with developing meiotic cells. However, it is difficult to make a conclusion at this time as to whether the delayed development in two central layers is an overall effect or is caused by defects in certain critical events such as cytokinesis.

In order to address these questions, it will be helpful to continue with additional genetic studies. The intermediate phenotype of *ems1-2 serk1-1* is ideal for genetic screening to identify downstream signaling molecules which may cause irreversible fertility loss in the *ems1-2 serk1-1* background.

Chapter 5 Conclusions and Future Directions

5.1 Conclusion

In this study, we proposed that SERK1/2 work as co-receptors of EMS1 during anther cell development in *Arabidopsis*.

In our genetic studies, we demonstrated that *SERK1/2* genetically interact with *EMS1*, showing additive effect in the *ems1-2* weak allele background. Meanwhile, *EMS1* signaling requires the normal function of *SERK1/2*. We also showed that *SERK1/2* play redundant but unequally important roles in the *EMS1* signaling pathway.

For biochemical approaches, we mainly used the BiFC system for the interaction tests in *Arabidopsis* protoplasts. We observed specific interaction between full length EMS and SERK1, which was not affected by the absence of TPD1. We also observed specific interaction between truncated EMS and SERK1 proteins including only LRR and transmembrane domains. Furthermore, we detected homodimerization between SERK1, but not EMS1.

In our functional analysis of EMS1 phosphorylation, we examined transphosphorylation between GST-EMS1-KD and His-SERK1-KD proteins, and observed the enhanced phosphorylation levels on both proteins as the effect of transphosphorylation. We then introduced mutations to both proteins, trying to abolish their autophosphorylation activities. Multiple phosphorylation sites were identified on

serine/threonine residues within the kinase domain from GST-EMS1-KD samples after in vitro kinase assay treatment.

5.2 Directions for future studies

For future continuation of this study, the following genetic and biochemical approaches can be used.

Genetically, the next major breakthrough that can be predicted would be the discovery of new signaling molecules in the EMS1 signaling pathway. As previously mentioned, the intermediate and reversible sterile phenotype of *ems1-2 serk1-1* is ideal material for genetic enhancer or suppressor screening

For biochemical studies, more examination can be performed using the BiFC system, such as further tests using truncated proteins without LRR domains or with only partial LRR domains. Stronger evidence will also be obtained upon the completion of our ongoing coimmunoprecipitation work.

For functional analysis of EMS1 phosphorylation, transphosphorylation between kinase active and inactive EMS1 and SERK1 proteins can be examined if our mutagenesis effort within the EMS1 activation loop turns out to be fruitful.

We are also testing the physiological importance of identified phosphorylation sites in *Arabidopsis*. For this purpose, corresponding mutations will be introduced into full length EMS1 for complementation tests.

Another powerful tool will be the dissection of EMS1 functional domains using both computational and biophysical methods. We may shift future research direction in order to address some questions that cannot be answered by methods currently used.

References

- Albrecht, C., Russinova, E., Hecht, V., Baaijens, E., and de Vries, S.C.** (2005) The *Arabidopsis thaliana* SOMATIC EMBRYOGENESIS RECEPTOR-LIKE KINASES1 and 2 control male sporogenesis. *Plant Cell* **17**: 3337–3349.
- Albrecht, C., Russinova, E., Kemmerling, B., Kwaaitaal, M., and de Vries, S.C.** (2008). *Arabidopsis* SOMATIC EMBRYOGENESIS RECEPTOR KINASE proteins serve brassinosteroid-dependent and -independent signaling pathways. *Plant Physiol.* **148**: 611–619.
- Bleckmann, A., Weidtkamp-Peters, S., Seidel, C.A.M., and Simon, R.** (2010). Stem cell signaling in *Arabidopsis* requires CRN to localize CLV2 to the plasma membrane. *Plant Physiol.* **152**: 166–176.
- Bowman, J.L., Smyth, D.R., and Meyerowitz, E.M.** (1989). Genes directing flower development in *Arabidopsis*. *Plant Cell* **1**: 37-52.
- Bowman, J.L., Drews, G.N., and Meyerowitz, E.M.** (1991a). Expression of the *Arabidopsis* floral homeotic gene AGAMOUS is restricted to specific cell types late in flower development. *Plant Cell* **3**: 749-758.
- Bowman, J.L., Smyth, D.A., and Meyerowitz, E.M.** (1991b). Genetic interactions among floral homeotic genes of *Arabidopsis*. *Development* **112**: 1-20.

- Bowman, J.L., Alvarer, J., Weigel, D., Meyerowitz, E.M., and Smyth, D.R.** (1993). Control of flower development in *Arabidopsis thaliana* by APETALA7 and interacting genes. *Development* **119**: 721-743.
- Canales, C., Bhatt, A.M., Scott, R., and Dickinson, H.** (2002). EXS, a putative LRR receptor kinase, regulates male germline cell number and tapetal identity and promotes seed development in *Arabidopsis*. *Curr. Biol.* **12**: 1718–1727.
- Caño-Delgado, A., Yin, Y., Yu, C., Vafeados, D., Mora-García, S., Cheng, J.C., Nam, K.H., Li, J., and Chory, J.** (2004). BRL1 and BRL3 are novel brassinosteroid receptors that function in vascular differentiation in *Arabidopsis*. *Development* **131**: 5341–5351.
- Chinchilla, D., Zipfel, C., Robatzek, S., Kemmerling, B., Nürnberger, T., Jones, J.D.G., Felix, G., and Boller, T.** (2007). A flagellin-induced complex of the receptor FLS2 and BAK1 initiates plant defence. *Nature* **26**: 497–500.
- Clark, S.E., Williams, R.W., and Meyerowitz, E.M.** (1997). The CLAVATA1 gene encodes a putative receptor kinase that controls shoot and floral meristem size in *Arabidopsis*. *Cell* **89**:575–585.
- Clough, S.J., and Bent, A.F.** (1998). Floral dip: A simplified method for *Agrobacterium*-mediated transformation of *Arabidopsis thaliana*. *Plant J.* **16**: 735–743.
- Colcombet, J., Boisson-Dernier, A., Ros-Palau, R., Vera, C.E., and Schroeder, J.I.** (2005). *Arabidopsis* SOMATIC EMBRYOGENESIS RECEPTOR KINASES1 and 2 are essential for tapetum development and microspore maturation. *Plant Cell* **17**: 3350–3361.

DeYoung, B. J., Bickle, K. L., Schrage, K.J., Muskett, P., Patel, K., and Clark, S. E. (2006). The CLAVATA1-related BAM1, BAM2 and BAM3 receptor kinase-like proteins are required for meristem function in Arabidopsis. *Plant J.* **45**: 1–16.

Domagalska, M.A., Schomburg, F.M., Amasino, R.M., Vierstra, R.D., Nagy, F., and Davis, S.J. (2007). Attenuation of brassinosteroid signaling enhances FLC expression and delays flowering. *Development* **134**: 2841–2850.

Earley, K.W., Haag, J.R., Pontes, O., Opper, K., Juehne, T., Song, K., and Pikaard, C.S. (2006). Gateway-compatible vectors for plant functional genomics and proteomics. *Plant J.* **45**: 616–629.

Goldberg, R.B., Beals, T.P., and Sanders, P.M. (1993). Anther development: Basic principles and practical applications. *Plant Cell* **5**:1217–1229.

Gómez-Gómez, L., and Boller, T. (2000). FLS2: An LRR receptor-like kinase involved in the perception of the bacterial elicitor flagellin in Arabidopsis. *Mol. Cell.* **5**:1003–1011.

Goto, K., and Meyerowitz, E.M. (1994). Function and regulation of the Arabidopsis floral homeotic gene PISTILLATA. *Genes Dev.* **8**: 1548–1560.

He, K., Gou, X., Yuan, T., Lin, H., Asami, T., Yoshida, S., Russell, S.D., and Li, J. (2007). BAK1 and BKK1 regulate brassinosteroid-dependent growth and brassinosteroid-independent cell-death pathways. *Curr. Biol.* **17**: 1109–1111

Hecht, V., Velle-Calzada, J.P., von Recklinghuasen, L., Hartog, M.V., Zwartjes, C., Schmidt, E.D.L., Boutilier, K., Grossniklaus, U., and de Vries, S.C. (2001). The Arabidopsis SOMATIC EMBRYOGENESIS RECEPTOR KINASE 1 gene is expressed in developing ovules and embryos and enhances embryogenic competence in culture. *Plant Physiol* **127**: 803–816.

Heese, A., Hann, D.R., Gimenez-Ibanez, S., Jones, A.M., He, K., Li, J., Schroeder, J.I., Peck, S.C., and Rathjen, J.P. (2007). The receptor-like kinase SERK3/BAK1 is a central regulator of innate immunity in plants. *Proc. Natl. Acad. Sci. USA* **104**: 12217–12222.

Hord, C. L. H., Chen, C. B., DeYoung, B. J., Clark, S. E. and Ma, H. (2006). The BAM1/BAM2 receptor-like kinases are important regulators of Arabidopsis early anther development. *Plant Cell* **18**: 1667-1680.

Hothorn, M., Belkhadir, Y., Dreux, M., Dabi, T., Noel, J.P., Wilson, I.A., and Chory, J. (2011). Structural basis of steroid hormone perception by the receptor kinase BRI1. *Nature* **474**: 467–471.

Ito, T., Wellmer, F., Yu, H., Das, P., Ito, N., Alves-Ferreira, M., Riechmann, J.L., and Meyerowitz, E.M. (2004). The homeotic protein AGAMOUS controls microsporogenesis by regulation of SPOROCTELESS. *Nature* **430**: 356–360.

Jack, T., Brockman, L.L., and Meyerowitz, E.M. (1992). The homeotic gene APETALA3 of Arabidopsis thaliana encodes a MADS box and is expressed in petals and stamens. *Cell* **68**: 683–697.

Jack, T., Fox, G.L., and Meyerowitz, E.M. (1994). Arabidopsis homeotic gene APETALA3 ectopic expression: Transcriptional and posttranscriptional regulation determine floral organ identity. *Cell* **76**: 703–716.

Jaillais, Y., Hothorn, M., Belkhadir, Y., Dabi, T., Nimchuk, Z.L., Meyerowitz, E.M., and Chory, J. (2011). Tyrosine phosphorylation controls brassinosteroid receptor activation by triggering membrane release of its kinase inhibitor. *Genes Dev.* **25**: 232–237.

Jia, G.X., Liu, X.D., Owen, H. A. and Zhao, D.Z. (2008). Signaling of cell fate determination by the TPD1 small protein and EMS1 receptor kinase. *Proc. Natl. Acad. Sci. USA* **105**: 2220-2225.

Jinn, T.L., Stone, J.M., and Walker, J.C. (2000). HAESA, an Arabidopsis leucine-rich repeat receptor kinase, controls floral organ abscission. *Genes Dev.* **14**:108–117.

Karlova, R., Boeren, S., van Dongen, W., Kwaaitaal, M., Aker, J., Vervoort, J., and de Vries, S.C. (2009). Identification of in vitro phosphorylation sites in the Arabidopsis thaliana somatic embryogenesis receptor-like kinases. *Proteomics* **9**: 368–379.

Kemmerling, B., Schwedt, A., Rodriguez, P., Mazzotta, S., Frank, M., Qamar, S.A., Mengiste, T., Betsuyaku, S., Parker, J.E., Müssig, C., Thomma, B., Albrecht, C., de Vries, S.C., Hirt, H., and Nürnberger, T. (2007). The BRI1-associated kinase 1, BAK1, has a brassinolide-independent role in plant cell-death control. *Curr. Biol.* **17**: 1116–1122.

Kinoshita, A., Betsuyaku, S., Osakabe, Y., Mizuno, S., Nagawa, S., Stahl, Y., Simon, R., Yamaguchi-Shinozaki, K., Fukuda, H., and Sawa, S. (2010). RPK2 is an essential receptor-like kinase that transmits the CLV3 signal in Arabidopsis. *Development* **137**: 3911–3920.

Krizek, B.A., and Meyerowitz, E.M. (1996). The Arabidopsis homeotic genes APETALA3 and PISTILLATA are sufficient to provide the B class organ identity function. *Development* **112**: 11–22.

Li, J., and Chory, J. (1997). A putative leucine-rich repeat receptor kinase involved in brassinosteroid signal transduction. *Cell* **90**:929–938.

Li, J., Wen, J., Lease, K.A., Doke, J.T., Tax, F.E., and Walker, J.C. (2002). BAK1, an Arabidopsis LRR receptor-like protein kinase, interacts with BRI1 and modulates brassinosteroid signaling. *Cell* **110**: 213–222.

Lohmann, J.U., Hong, R.L., Hobe, M., Busch, M.A., Parcy, F., Simon, R., and Weigel, D. (2001). A molecular link between stem cell regulation and floral patterning in Arabidopsis. *Cell* **105**: 793–803

Ma, H. (2005). Molecular genetic analyses of microsporogenesis and microgametogenesis in flowering plants. *Annu. Rev. Plant Biol.* **56**:393–434.

Mizuno, S., Osakabe, Y., Maruyama, K., Ito, T., Osakabe, K., Sato, T., Shinozaki, K., and Yamaguchi-Shinozaki, K. (2007). Receptor-like protein kinase 2 (RPK 2) is a novel factor controlling anther development in Arabidopsis thaliana. *Plant J.* **50**: 751-766.

- Müller, R., Bleckmann, A. and Simon, R.** (2008). The receptor kinase CORYNE of Arabidopsis transmits the stem cell-limiting signal CLAVATA3 independently of CLAVATA1. *Plant Cell* **20**: 934-946.
- Nakagawa, T., Kurose, T., Hino, T., Kawamukai, M., Niwa, N., Toyooka, K., Matsuoka, K., Jinbo, T., and Kimura, T.** (2007). Development of series of gateway binary vectors, pGWBs, for realizing efficient construction of fusion genes for plant transformation. *J. Biosci. Bioeng.* **104**: 33–41.
- Nam, K.H., and Li, J.** (2002). BRI1/BAK1, a receptor kinase pair mediating brassinosteroid signaling. *Cell* **110**: 203–212.
- Oh, M.H., Ray, W.K., Huber, S.C., Asara, J.M., Gage, D.A., and Clouse, S.D.** (2000). Recombinant brassinosteroid insensitive 1 receptor-like kinase autophosphorylates on serine and threonineresidues and phosphorylates a conserved peptide motif in vitro. *Plant Physiol.* **124**: 751–766.
- Oh, M.H., Wang, X., Kota, U., Goshe, M.B., Clouse, S.D., and Huber, S.C.** (2009). Tyrosine phosphorylation of the BRI1 receptor kinase emerges as a component of brassinosteroid signaling in Arabidopsis. *Proc. Natl. Acad. Sci. USA* **106**: 658–663.
- Oh, M.H., Wang, X., Wu, X., Zhao, Y., Clouse, S.D., and Huber, S.C.** (2010). Autophosphorylation of Tyr-610 in the receptor kinase BAK1 plays a role in brassinosteroid signaling and basal defense gene expression. *Proc. Natl. Acad. Sci. USA* **107**: 17827–17832.
- Ohad, N., Shichrur, K., and Yalovsky, S.** (2007). The analysis of protein-protein interactions in plants by bimolecular fluorescence complementation. *Plant Physiol.* **145**: 1090–1099.

Rojo, E., Sharma, V.K., Kovaleva, V., Raikhel, N.V., and Fletcher, J.C. (2002). CLV3 is localized to the extracellular space, where it activates the Arabidopsis CLAVATA stem cell signaling pathway. *Plant Cell* **14**: 969–977.

Sanders, P.M., Ansthu, Q.B., Weterings, K., McIntire, K.N., Hsu, Y., Lee, P.Y., Truong, M.T., Beals, T.P., and Goldberg, R.B. (1999). Anther developmental defects in Arabidopsis thaliana male-sterile mutants. *Sex. Plant Reprod.* **11**: 297–322.

Santiago, J., Henzler, C., and Hothorn, M. (2013). Molecular mechanism for plant steroid receptor activation by somatic embryogenesis co-receptor kinases. *Science* **341**: 889-892.

Schiefthaler, U., Balasubramanian, S., Sieber, P., Chevalier, D., Wisman, E., and Schneitz, K. (1999). Molecular analysis of NOZZLE, a gene involved in pattern formation and early sporogenesis during sex organ development in Arabidopsis thaliana. *Proc. Natl. Acad. Sci. USA* **96**: 11664–11669.

Scott, R.J., Spielman, M., and Dickinson, H.G. (2004) Stamen structure and function. *Plant Cell* **16** :S46–S60.

Sheridan, W.F., Golubeva, E.A., Abrhamova, L.I., Golubovskaya, I.N. (1999). The macl mutation alters the developmental fate of the hypodermal cells and their cellular progeny in the maize anther. *Genetics* **153**:933–941.

Shiu, S.H., and Blecker, A.B. (2001). Receptor-like kinases from Arabidopsis form a monophyletic gene family related to animal receptor kinases. *Proc. Natl. Acad. Sci. USA* **98**: 10763–10768.

- Sun, W., Cao, Y., Jansen, K.L., Bittel, P., Boller, T., and Bent, A.F.** (2012). Probing the Arabidopsis flagellin receptor: FLS2–FLS2 association and the contributions of specific domains to signaling function. *Plant Cell* **24**: 1096–1113.
- Torii, K.U., Mitsukawa, N., Oosumi, T., Matsuura, Y., Yokoyama, R., Whittier, R.F., and Komeda, Y.** (1996). The Arabidopsis ERECTA gene encodes a putative receptor protein kinase with extracellular leucine-rich repeats. *Plant Cell* **8**: 735–746.
- Torii, K.U.** (2004) Leucine-rich repeat receptor kinases in plants: structure, function, and signal transduction pathways. *Int. Rev. Cytol.* **234**:1–46.
- Tzfira, T., Tian, G.W., Lacroix, B.T., Vyas, S., Li, J., Leitner-Dagan, Y., Krichevsky, A., Taylor, T., Vainstein, A., and Citovsky, V.** (2005). pSAT vectors: A modular series of plasmids for fluorescent protein tagging and expression of multiple genes in plants. *Plant Mol. Biol.* **57**: 503–516.
- Trotochaud, A., Jeong, S., and Clark, S.E.** (2000). CLAVATA3, a multimeric ligand for the CLAVATA1 receptor-kinase. *Science* **289**: 613–617.
- Walter, M., Chaban, C., Schutze, K., Batistic, O., Weckermann, K., Nake, C., Blazevic, D., Grefen, C., Schumacher, K., Oecking, C., Harter, K., and Kudla, J.** (2004). Visualization of protein interactions in living plant cells using bimolecular fluorescence complementation. *Plant J.* **40**: 428–438.
- Wang, X.L., Goshe, M.B., Soderblom, E.J., Phinney, B.S., Kuchar, J.A., Li, J., Kinoshita, T., Cano-Delgado, A., Seto, H., Hiranuma, S., Fujioka, S., Yoshida, S., and Chory, J.** (2005). Binding of brassinosteroids to the extracellular domain of plant receptor kinase BRI1. *Nature* **433**: 167–171.

- Wang, X.L and Chory, J.** (2006). Brassinosteroids regulate dissociation of BKI1, a negative regulator of BRI1 signaling, from the plasma membrane. *Science* **313**: 1118–1122.
- Wang, X.F., Goshe, M.B., Soderblom, E.J., Phinney, B.S., Kuchar, J.A., Li, J., Asami, T., Yoshida, S., Huber, S.C., and Clouse, S.D.** (2005). Identification and functional analysis of in vivo phosphorylation sites of the Arabidopsis BRASSINOSTEROID-INSENSITIVE1 receptor kinase. *Plant Cell* **17**: 1685–1703.
- Wang, X.F., Kota, U., He, K., Blackburn, K., Li, J., Goshe, M.B., Huber, S.C., Clouse, S.D.** (2008) Sequential transphosphorylation of the BRI1/BAK1 receptor kinase complex impacts early events in brassinosteroid signaling. *Dev. Cell* **15**: 220–235
- Weigel, D., and Meyerowitz, E.M.** (1994). The ABCs of floral homeotic genes. *Cell* **78**: 203–209.
- Wijeratne, A.J., Zhang, W., Sun, Y., Liu, W., Albert, R., Zheng, Z., Oppenheimer, D.G., Zhao, D.Z., and Ma, H.** (2007). Differential gene expression in Arabidopsis wild-type and mutant anthers: insights into anther cell differentiation and regulatory networks. *Plant J.* **52**, 14-29.
- Yang, S. L., Jiang, L. X., Pua, C. S., Xie, L. F., Zhang, X. Q., Chen, L. Q., Yang, W. C. and Ye, D.** (2005). Overexpression of Tapetum determinant1 alters the cell fates in the Arabidopsis carpel and tapetum via genetic interaction with excess microsporocytes1/extra sporogenous cells. *Plant Physiol.* **139**: 186-191.

Yang, S.Y., Xie, L.F., Mao, H.Z., Puah, C.P., Yang, W.C., Jiang, L., Sundaresan, V., and Ye, D. (2003). TAPETUM DETERMINANT1 is required for cell specialization in the Arabidopsis anther. *Plant Cell* **15**: 2792–2804.

Yang, W.C., Ye, D., Xu, J., and Sundaresan, V. (1999). The SPOROCTELESS gene of Arabidopsis is required for initiation of sporogenesis and encodes a novel nuclear protein. *Genes Dev.* **13**: 2108–2117.

Zhao, D.Z., Wang, G.W., Speal, B., and Ma, H. (2002). The EXCESS MICROSPOROCTES1 gene encodes a putative leucine-rich repeat receptor protein kinase that controls somatic and reproductive cell fate in the Arabidopsis anther. *Genes Dev* **16**: 2021–2031.

Zhao, X., de Palma, J., Oane, R., Gamuyao, R., Luo, M., Chaudhury, A., Hervé P., Xue, Q., Bennett, J. (2008). OsTDL1A binds to the LRR domain of rice receptor kinase MSP1, and is required to limit sporocyte numbers. *Plant J.* **54**: 375–387.

Zhu, Y., Wang, Y., Li, R., Song, X., Wang, Q., Huang, S., Jin, J. B., Liu, C. M. and Lin, J. (2009). Analysis of interactions among the CLAVATA3 receptors reveals a direct interaction between CLAVATA2 and CORYNE in Arabidopsis. *Plant J.* **61**: 223-233.

CURRICULUM VITAE

Yao Wang

3209 N.Maryland Ave, Lapham Hall S181

Milwaukee, WI, 53211

yaowang@uwm.edu

Education:

2007-present: **Ph.D. Biological Sciences**

University of Wisconsin-Milwaukee

2003-2007: **B.S. Biological Sciences**

Nanjing Normal University, Nanjing, China

Research Experience:

2007-present: University of Wisconsin-Milwaukee, Lab of Dr. Da-Zhong Zhao

Graduate student researcher

2005-2007: Jiang Su Province Key Laboratory for Molecular and Medical Biotechnology,
Life Science College, Nanjing Normal University

Lab of Dr.Chao-Jun Li and Hua-Qun Chen

Undergraduate Research Assistant

Publications:

Liu, X.D., Huang, J., **Wang, Y.**, Khanna, K., Xie, Z.X., Owen, H.A., Zhao, D.Z. (2010).

The role of floral organs in carpels, an Arabidopsis loss-of-function mutation in microRNA160a, in organogenesis and the mechanism regulating its expression.

Plant J. **62**: 416–428.